

## Angular-Correlation Measurements and the $\text{Si}^{30}(p,\gamma)\text{P}^{31}$ Reaction

GALE I. HARRIS AND D. V. BREITENBECHER

*Aerospace Research Laboratories,\* Wright-Patterson Air Force Base, Ohio*

(Received 2 December 1965; revised manuscript received 13 January 1966)

Gamma-ray angular-distribution and triple-correlation measurements have been performed at the  $E_p=1095$ -,  $1204$ -, and  $1322$ -keV resonances in the  $\text{Si}^{30}(p,\gamma)\text{P}^{31}$  reaction which provide new information on properties of the  $E_x=3.29$ -,  $3.51$ -,  $4.26$ -, and  $4.63$ -MeV levels of  $\text{P}^{31}$ . The angular-correlation data have been analyzed with newly developed search programs which utilize the substate population representation and a recently introduced factored form of the correlation functions which is applicable to multiple cascades. The previous assignments  $3.29$  ( $\frac{5}{2}$ ),  $3.51$  ( $\frac{3}{2}$ ), and  $4.26$  ( $\frac{3}{2}$ ) are confirmed, and  $J=\frac{3}{2}$  is assigned to the  $4.63$ -MeV level. The  $3.29$ -MeV level decays in the ratio  $77:23$  to the  $1.27$ - and  $2.23$ -MeV levels. No evidence is found for the previously reported  $3.29 \rightarrow 0$  transition. The quadrupole-dipole amplitude ratios ( $\delta$ ) for the  $3.29 \rightarrow 1.27$  and  $3.29 \rightarrow 2.23$  transitions are  $-0.44 \pm 0.02$  and  $-0.41 \pm 0.06$ , respectively. The value of  $\delta$  for the  $3.51 \rightarrow 0$  transition is  $-0.41 \pm 0.03$  or  $7.1 \pm 1.0$ . The  $3.51$ -MeV level was also found to decay to both the first- and second-excited states and unambiguous values for the mixing ratios were obtained. The  $4.26$ -MeV level was found to decay in the ratio  $76:20:4$  to the ground, first-excited, and second-excited states. The  $4.63$ -MeV level was found to decay in the ratio  $27:52:21$  to the same states. A new decay scheme is proposed for the  $E_p=1095$ -keV resonance which proved to be more complex than had been previously reported. The values of  $\delta$  obtained for the  $4.26 \rightarrow 0$ ,  $4.26 \rightarrow 1.27$ ,  $4.63 \rightarrow 0$ , and  $4.63 \rightarrow 1.27$  transitions are  $-0.32 \pm 0.04$  or  $4.7 \pm 0.9$ ,  $-0.25 \pm 0.05$ ,  $0.07 \pm 0.04$  or  $1.48 \pm 0.12$ , and  $-0.02 \pm 0.05$  or  $-3.9 \pm 1.0$ , respectively. All the ambiguities in  $\delta$ , except for the last one, are due to inherent limitations in the intensity-direction correlation method. The extended version of the triple-correlation formulation for multiple cascades was found to be very useful in some of the more complex situations encountered in this work. A brief review of recent model calculations which relate to properties of states in  $\text{P}^{31}$  is given. On the basis of comparison of results of available calculations, it appears that the weak-coupling unified models receive the most support from the existing data.

### INTRODUCTION

THE location of the bound energy levels of  $\text{P}^{31}$  up through the excitation energy of  $5.01$  MeV has been known since the precision, inelastic proton-scattering work of Endt and Paris.<sup>1</sup> The determination of the spins, parities, and detailed decay properties of these bound states has since been the object of several intensive studies including the proton-capture work of Hoogenboom<sup>2</sup>, Broude, Green, and Willmott<sup>3</sup>; Harris and Seagondollar<sup>4,5</sup> (referred to as I and II); and Van Rinsvelt and Smith.<sup>6</sup> The status of this work as of 1962 is reviewed by Endt and Van der Leun.<sup>7</sup> Progress since that review has included the assignment of spin  $\frac{1}{2}$  instead of  $\frac{3}{2}$  to the  $3.13$ -MeV level,<sup>8</sup> the assignment of  $\frac{7}{2}$  to the  $3.41$ -MeV level,<sup>5,6</sup> an assignment confirmed in the present work of  $\frac{3}{2}$  to the  $4.26$ -MeV level,<sup>5</sup> and the assignment of  $\frac{7}{2}$  to the  $4.43$ -MeV level.<sup>9</sup> In addition, revisions in the decay schemes of the  $3.41$ -,  $3.51$ -,  $4.26$ -,  $4.43$ -, and  $5.01$ -MeV levels have been found necessary.<sup>4,6,9</sup>

The existence of several bound states above  $E_x=5.01$  MeV is suggested by the proton capture work,<sup>2-4</sup> high-energy electron and proton scattering work,<sup>10,11</sup> and recently, several levels have been found by  $17.5$ -MeV inelastic proton scattering measurements<sup>12</sup> and by means of the  $\text{Si}^{30}(d,n)\text{P}^{31}$  reaction.<sup>13</sup> Information on the electromagnetic transition properties of some of these new levels, in addition to some of those below  $5.01$  MeV, has been gained from the high-energy scattering studies. In addition, a new first-excited state has been proposed at  $E_x=0.45$  MeV from studies of the  $\text{S}^{32}(n,d)\text{P}^{31}$  reaction.<sup>14</sup> However, no confirmation of such a level has been obtained in subsequent work,<sup>13</sup> and it seems highly improbable that a level at this energy would not have been populated by decays from the more than forty well-studied resonance states formed in the proton-capture reaction.

The present paper reports results of directional-correlation and spectroscopic measurements on gamma-ray transitions from resonances in the  $\text{Si}^{30}(p,\gamma)\text{P}^{31}$  reaction formed with bombarding energies between  $1.0$  and  $1.5$  MeV. Specific emphasis is placed on the determination of properties of the bound states at  $E_x=3.29$ ,  $3.51$ ,  $4.26$ , and  $4.63$  MeV excited via cascades from the

\* An element of the Office of Aerospace Research, U. S. Air Force.

<sup>1</sup> P. M. Endt and C. H. Paris, Phys. Rev. **106**, 764 (1957).

<sup>2</sup> A. M. Hoogenboom, thesis, University of Utrecht, 1958 (unpublished).

<sup>3</sup> C. Broude, L. L. Green, and J. C. Willmott, Proc. Phys. Soc. (London) **72**, 1097 (1958).

<sup>4</sup> G. I. Harris and L. W. Seagondollar, Phys. Rev. **128**, 338 (1962).

<sup>5</sup> G. I. Harris and L. W. Seagondollar, Phys. Rev. **131**, 787 (1963).

<sup>6</sup> H. Van Rinsvelt and P. B. Smith, Physica **30**, 59 (1964).

<sup>7</sup> P. M. Endt and C. Van der Leun, Nucl. Phys. **34**, 1 (1962).

<sup>8</sup> H. Van Rinsvelt and P. M. Endt, Phys. Letters **9**, 266 (1964).

<sup>9</sup> G. I. Harris, H. J. Hennecke, and F. W. Prosser, Jr., Phys. Letters **9**, 324 (1964).

<sup>10</sup> P. Kossanyi-Demay, R. M. Lombard, and G. R. Bishop, Nucl. Phys. **62**, 615 (1965).

<sup>11</sup> J. C. Jacmart, M. Liu, R. A. Ricci, M. Riou, and C. Ruhla, Phys. Letters **8**, 273 (1964).

<sup>12</sup> G. M. Crawley and G. T. Garvey, Bull. Am. Phys. Soc. **10**, 526 (1965), also, G. M. Crawley, thesis, Princeton University, 1965 (unpublished).

<sup>13</sup> B. Cujec, W. G. Davies, W. K. Dawson, T. B. Grandy, G. C. Neilson, and K. Ramavatavam, Phys. Letters **15**, 266 (1965).

<sup>14</sup> L. Colli, P. Forti, and E. Gadioli, Nucl. Phys. **54**, 253 (1964).

resonances at  $E_p=1095$ , 1204, and 1322 keV. The spins and decay properties of these resonances have been reported earlier.<sup>4-6</sup> The measurements discussed here yield new information on the spins, decay schemes, and multipolarity mixings of transitions of the indicated bound states. A subsequent report will describe in greater detail measurements at the  $E_p=2187$ -keV resonance with yield information on the 9.42- and 4.43-MeV levels. An angular-correlation analysis technique is introduced which takes advantage of the factored form of the triple-correlation functions and the more efficient computer search programs which result.<sup>15</sup> A discussion and comparison of existing data on  $P^{31}$  levels with results of recent model calculations is given in the final section.

### EXPERIMENTAL PROCEDURE

The  $\text{Si}^{30}(p,\gamma)\text{P}^{31}$  reaction was induced by a magnetically analyzed beam of protons from the Aerospace Research Laboratory (ARL) 2-MeV Van de Graaff accelerator. The essential features of the beam-handling system and target preparation and cooling techniques have been discussed in I and II. The presence of a liquid-nitrogen cold trap directly ahead of the target chamber and a liquid-nitrogen-trapped diffusion pump within about four feet of the target sufficed to keep the buildup of carbon and fluorine on the target at a very low level. Most of the measurements were performed with 7-10  $\mu\text{A}$  beam currents collimated and focused to an approximately 3-mm diam spot size at the target. The beam-energy resolution was generally about 1 keV for this work, and it was found that adjustments in beam energy were rarely required to remain on the narrow resonances involved.

The angular distribution measurements were performed with a 5-in.-diam  $\times$  5-in.-long NaI(Tl) detector as described in II. Some of the earlier triple-correlation measurements were also performed with the setup described in II; namely, an 8-in.-diam  $\times$  8-in.-long NaI(Tl) detector fixed at the angles  $\theta=90^\circ$  and  $\phi=90^\circ$  or  $180^\circ$ , and a 5-in.-diam  $\times$  5-in.-long detector movable between  $\theta=0^\circ$  and  $90^\circ$  ( $\phi=0^\circ$ ) in a polar coordinate system with  $Z$  axis along the beam propagation direction. A later, much more efficient arrangement, used for most measurements reported here, consisted of two fixed 5-in.  $\times$  5-in. detectors, a movable 8-in.  $\times$  8-in. detector with provisions for coincidence between its output pulses and those from either of the fixed 5-in.  $\times$  5-in. detectors, and a "truncated-wedge" shaped crystal used as a monitor. A schematic drawing of this arrangement is shown in Fig. 1. It was usually possible with this system to measure "simultaneously" four triple-correlation geometries on a given double cascade in the course of one "pass" of the movable detector (C) between  $\theta_V=0^\circ$  and  $90^\circ$ . In practice, a minimum of

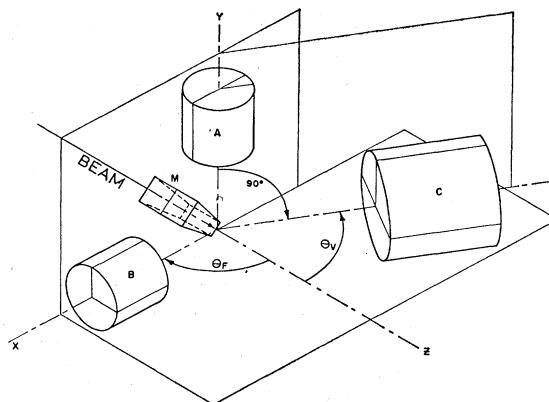


FIG. 1. Diagram of detector arrangement used for triple-correlation measurements. Pulses derived from the 5-in. long  $\times$  5-in. diam NaI(Tl) detectors labeled A and B are used to gate a multi-channel analyzer which records the spectrum of pulses from the 8-in. long  $\times$  8-in. diam detector labeled C. The reaction was monitored by detector M. Detector A was located vertically above the target, and detector B was normally located at  $\theta_F=90^\circ$  or  $135^\circ$  in the present work. The angle  $\theta_V$  was varied between  $0^\circ$  and  $90^\circ$  as discussed in the text. The incoming beam lies along the  $Z$  axis.

two such passes with angular settings (usually) of  $\theta_V=0^\circ, 30^\circ, 45^\circ, 60^\circ,$  and  $90^\circ$  in random sequence were made in order to minimize the possible effects of systematic drifts in electronics, target contamination buildup, etc. Such effects were generally found to be not very significant in comparison with the random counting errors. One of the fixed detectors (A) was always located directly above the target at  $\theta=\phi=90^\circ$ , and the other (B) in the horizontal plane at either  $\theta_F=90^\circ, \phi=180^\circ$  or  $\theta_F=135^\circ, \phi=180^\circ$ . The latter position was used in some cases to take advantage of the odd- $N$  dependence of the angle factor  $X_{KM}^N(\theta_1, \theta_2, \phi)$  in the triple-correlation functions.

The pulses from the detectors were amplified and shaped by White, cathode-follower preamplifiers and double delay-line amplifiers. The detector systems were gain-stabilized with commercial stabilizers using the 0.662-MeV  $\text{Cs}^{137}$  gamma ray as a reference. The amplified pulses from each of the detectors (A and B) entered two single-channel analyzers which furnished gate and route pulses for a 512-channel analyzer. In this manner, the amplified pulses from detector (C) were stored in four separate sections of the memory of the 512-channel analyzer; thus giving four coincidence spectra for each angular setting. Some variations of this basic procedure were used and will be mentioned, where significant, in the discussion of specific measurements. The accumulated spectra were then usually transferred to another 512-channel analyzer via punched paper tape. The second analyzer then provided typewriter and X-Y plotter readout service while the next data run was in progress.

The target chamber and detector system was checked for asymmetry using the known isotropic radiation from the  $E_p=620$  keV resonance in the

<sup>15</sup> G. I. Harris, H. J. Hennecke, and D. D. Watson, Phys. Rev. 139, B1113 (1965).

$\text{Si}^{30}(p,\gamma)\text{P}^{31}$  reaction. Corrections were made to the data for these effects, if significant, and for any variation between runs of the monitor output. The monitor output was obtained from a single-channel analyzer set to accept pulses from a prominent line in the resonance decay spectrum. Monitor gain stabilization was used in all cases. Corrections were also made for chance coincidence rates where significant.

No special attempt was made to maintain normalization between the various triple-correlation geometries measured on a given cascade due to the somewhat unusual combination of several large detectors used in this work. Instead, the normalizations between triple-correlation geometries and angular distributions were treated, as discussed below, as adjustable parameters in the analysis.

#### ANALYSIS OF ANGULAR CORRELATION DATA

Most of the data presented in this paper were first analyzed by means of the same contour-diagram procedures used in II. In this method, the coefficients in a Legendre-polynomial representation of the correlation functions are determined by least-squares analysis of the data. These experimental coefficients are then compared with theoretically possible coefficients by a contour presentation in which the contours represent fixed values of the coefficients in the  $\delta_1, \delta_2$  plane. The variables  $\delta_1$  and  $\delta_2$  represent the multipolarity mixing ratios of the primary and secondary members, respectively, of the double cascade under observation. The requirement for an acceptable solution for a given spin combination is the mutual intersection of contours from the different experimental geometries measured.

The data were all subsequently reanalyzed using a radically different and much more efficient method which utilizes a new "factored" version of the triple-correlation formula and computer  $\chi^2$  search program techniques which result.<sup>15,16</sup> Reference 15 contains the general formulation and discussion of the analysis procedures used here, and Ref. 16 gives a more specific description of techniques used for the inclusion of angular distribution data, the treatment of errors, normalization procedures, and  $\chi^2$  analysis methods. The former reference introduces a generalized formulation of the triple-correlation problem which can be applied to multiple cascades which may involve one or more intermediate-unobserved radiations. Each radiation whether observed or not, is represented by a separate factor in the general formula which provides for more convenient application to specific problems and for efficient programming. Parallel formulations are given in terms of the population parameters and statistical tensors of the aligned state. In contrast with the earlier method mentioned above, the observed correlation intensity at each angular configuration of

detectors A and C (and/or B and C) were used as input data rather than polynomial expansion coefficients. The procedure has the advantage of uncorrelated input data and provides for a more straightforward least-squares analysis.<sup>17</sup>

The population-parameter representation was chosen for this work because the first-observed radiations of most cascades studied arose from resonance states which have only the  $m = \pm \frac{1}{2}$  substates populated in the reaction used. For completeness, we present the triple correlation formula of Ref. 15 specialized to the particular cases of this work. In the case of a double cascade between states with spin  $J_1, J_2, J_3$ , and no intermediate-unobserved radiations, we have for the intensity at an angular configuration denoted by  $a$

$$W_a = \sum_{mM} P(m) G_{mM}^a(\delta_1, \alpha) H_M(\delta_2, \beta), \quad (1)$$

where the  $P(m)$  represent the populations of the  $\pm m$  substates taken together and  $\alpha$  and  $\beta$  stand for the quantum numbers  $J_1, J_2$ , and  $J_2, J_3$ , respectively. The factor  $G_{mM}^a$  which relates to the first member of the cascade is given by

$$G_{mM}^a(\delta_1, \alpha) = \sum_{L_1 L_1'} (1 + \delta_1^2)^{-1} \delta_1^{p_1} \times \sum_{KN} E_{KM}^N(\alpha, L_1 L_1' m) Q_K Q_M X_{KM}^N(a), \quad (2)$$

where the  $Q_K$  and  $Q_M$  are factors which account for the finite size of the detectors (see II), and where the form of the angular function  $X_{KM}^N$  is standard.<sup>15,17</sup> The factor  $H_M$  which relates to the second member of the cascade is given by

$$H_M(\delta_2, \beta) = \sum_{L_2 L_2'} (1 + \delta_2^2)^{-1} \delta_2^{p_2} h_M(\beta, L_2, L_2'). \quad (3)$$

The coefficients  $E_{KM}^N$  and  $h_M$  of Eqs. (2) and (3) are defined in Ref. 15 and are tabulated<sup>18</sup> for multipolarities through octupole. The exponents  $p_1$  and  $p_2$  take on the values 0, 1, or 2 for pure  $L$ -pole, mixed  $L$ -,  $L'$ -pole, or pure  $L'$ -pole radiation, respectively.

Another special case encountered is one which involves a triple cascade between states with spins  $J_1, J_2, J_3, J_4$ , and where the  $J_2 \rightarrow J_3$  transition is unobserved. In this case, Eq. (1) still applies except that  $H_M$  is replaced by

$$\bar{H}_M(\delta_2, \delta_3, \beta, \gamma) = u_M(\delta_2, \beta) H_M(\delta_3, \gamma), \quad (4)$$

where  $\gamma$  stands for the quantum numbers  $J_3, J_4$ , and the factor  $u_M$  which relates to the unobserved radiation

<sup>17</sup> P. B. Smith, in *Nuclear Reactions*, edited by P. M. Endt and P. B. Smith (North-Holland Publishing Company, Amsterdam, 1962), Vol. II.

<sup>18</sup> D. D. Watson and G. I. Harris, Aerospace Research Laboratories Report No. ARL 66-0030, Wright-Patterson Air Force Base, Ohio (unpublished).

<sup>16</sup> D. D. Watson, G. I. Harris, and L. W. Seagondollar (to be published).

is given by<sup>15</sup>

$$u_M(\delta_2, \beta) = (1 + \delta_2^2)^{-1} [U_M(L_2\beta) + \delta_2^2 U_M(L_2'\beta)]. \quad (5)$$

The factors  $U_M$  are defined in Ref. 15 and are also tabulated.<sup>18,19</sup>

If the state denoted by  $J_1$  in these expressions is the resonance state formed by the  $\text{Si}^{30}(p, \gamma)\text{P}^{31}$  reaction, then only the  $m = \frac{1}{2}$  term appears in Eq. (1). Some triple correlations were performed in which  $J_1$  corresponds to the state formed by the emission of the first gamma ray of a triple cascade. In this case, terms other than those with  $m = \frac{1}{2}$  can appear in Eq. (1). The populations of state  $J_1$  depend upon the mixing  $\delta_p$  of the unobserved primary radiation as follows<sup>16,19</sup>:

$$P(m) = (1 + \delta_p^2)^{-1} [(Lm + \frac{1}{2}J_1 - m |J_{r\frac{1}{2}}|^2 + \delta_p^2 (L'm + \frac{1}{2}J_1 - m |J_{r\frac{1}{2}}|^2)], \quad (6)$$

where  $J_r$  is the spin of the resonance and  $L, L'$  are the multipolarities of the unobserved radiation.

The angular-distribution equations are a special case of the above formalism.<sup>16</sup> The distribution of the  $J_1 \rightarrow J_2$  transition is obtained by replacing  $Q_M$  of Eq. (2) by  $\delta_{M,0}$  which gives

$$W(\theta_1) = \sum_m P(m) \sum_{L_1 L_1'} (1 + \delta_1^2)^{-1} \delta_1^{2p_1} \times \sum_K E_{K0^0}(\alpha, L_1 L_1' m) Q_K X_{K0^0}(\theta_1). \quad (7)$$

Similarly, the distribution of the  $J_2 \rightarrow J_3$  transition is observed by setting  $Q_K = \delta_{K,0}$ , giving

$$W(\theta_2) = \sum_m P(m) \sum_{L_1 L_1'} (1 + \delta_1^2)^{-1} \delta_1^{2p_1} \times \sum_M E_{0M^0}(\alpha, L_1 L_1' m) H_M(\delta_2, \beta) Q_M X_{0M^0}(\theta_2). \quad (8)$$

The replacement of  $H_M$  in Eq. (8) by  $\bar{H}_M$  yields the  $J_3 \rightarrow J_4$  angular distribution. Equations (7) and (8) differ from the usual Legendre polynomial expressions only by the factors  $(2K+1)^{1/2}$  and  $(2M+1)^{1/2}$ , respectively.

The solution of Eq. (1) was accomplished using the "two-parameter method" of Ref. 15.<sup>20</sup> A computer program calculates by least-squares the best values of the set of  $P(m)$  of Eq. (1) for assigned values of the parameters  $\delta_1, \delta_2$  and the corresponding values of  $Q^2$  defined as

$$Q^2 = \frac{1}{A - P - q} \sum_a (W_a - W_a^*)^2 \omega_a^2, \quad (9)$$

where  $W_a^*$  is the value of  $W_a$  computed from Eq. (1) in which the least-square solutions for the  $P(m)$  have

<sup>19</sup> R. Nordhagen, Physics Institute, University of Oslo, 1964 (unpublished).

<sup>20</sup> For double cascades this method is essentially the same as that described by P. B. Smith [Can. J. Phys. **42**, 1101 (1964)] except for the computational advantages of the factored equations and the methods of presentation of the  $Q^2$  surfaces.

been resubstituted. The weight factor  $\omega_a$  is the inverse of the standard deviation of  $W_a$ ,  $A$  is the number of observation points,  $P$  is the number of population parameters, and  $q$  is the number of mixing parameters varied. The minimum value of  $Q^2$  is referred to as  $\chi^2$ . The condition  $P(m) \geq 0$  is automatically checked by the computer. If  $P(m) < 0$ , the computer recalculates the best set of  $P(m)$  with  $P(m) = 0$  and the corresponding new value of  $Q^2$ .

The program first computes and stores all  $H_M(\delta_2)$  for points equally spaced between  $\pm 90^\circ$  in the variable  $\tan^{-1} \delta_2$ . Then  $\tan^{-1} \delta_1$  is varied over the region from  $-90^\circ$  to  $90^\circ$  in equal sized steps and the quantities  $Q^2$ , the  $P(m)$ , and the corresponding error matrix are computed. The entire  $\delta_1, \delta_2$  plane is thereby covered by a grid typically as fine as  $2^\circ$  steps in  $\tan^{-1} \delta$  in a few minutes by an IBM 7094 computer. The output format used for the present work is as follows: For each fixed  $\delta_1$ , the  $\delta_2$  which corresponds to the minimum  $Q^2$  is located. This minimum  $Q^2$  and corresponding  $\delta_2$  value are printed out. Thus a projection in the  $Q^2, \delta_1$  plane of the three-dimensional  $Q^2$  surface is obtained. Similarly, a projection plot of the surface is obtained in the  $Q^2, \delta_2$  plane. The values of the  $P(m)$  and their error matrices are printed out for each point of the projection plots. It has been shown that errors in  $\delta_1$  or  $\delta_2$  obtained from the "width" of dips in the projection plots properly account for correlations between the two mixing ratios.<sup>16</sup>

As mentioned above, the data were taken in separate, unnormalized "geometries" in which two angles of the set  $(\theta_1, \theta_2, \phi)$  are held fixed and the third varied. (The angle  $\theta_1$  refers to the mean polar angle at which the first-observed member of the cascade is detected,  $\theta_2$  that for the second-observed member, and  $\phi$  the azimuthal angle between the two observed members.) For clarity, we introduce the following notation for the specification of geometries: The geometry in which, for example,  $\theta_1$  is fixed at  $90^\circ$ ,  $\theta_2$  is variable, and  $\phi$  is fixed at  $180^\circ$ , is designated by  $(90, V, 180)$ . This case has commonly been referred to as Geometry II in previous notations. If there is an unobserved radiation after the first but before the second observed radiation, then Geometry II would be designated by  $(90, u, V, 180)$ . The angular distributions of the first and second members of a cascade are referred to by AD1 and AD2, respectively.

The normalization factors for the separate geometries were treated as parameters which were determined by an iterative process in the analysis program.<sup>16</sup> The angular distributions were included on an equal footing as separate "geometries." This was accomplished by setting  $Q_M = \delta_{M,0}$  or  $Q_K = \delta_{K,0}$  in Eq. (2) for those points which belong to AD1 or AD2, respectively. It was always found that three iterations were sufficient to reach a stable minimum  $Q^2$  provided the input data were approximately normalized by estimation. The finite-geometry correction factors were obtained from

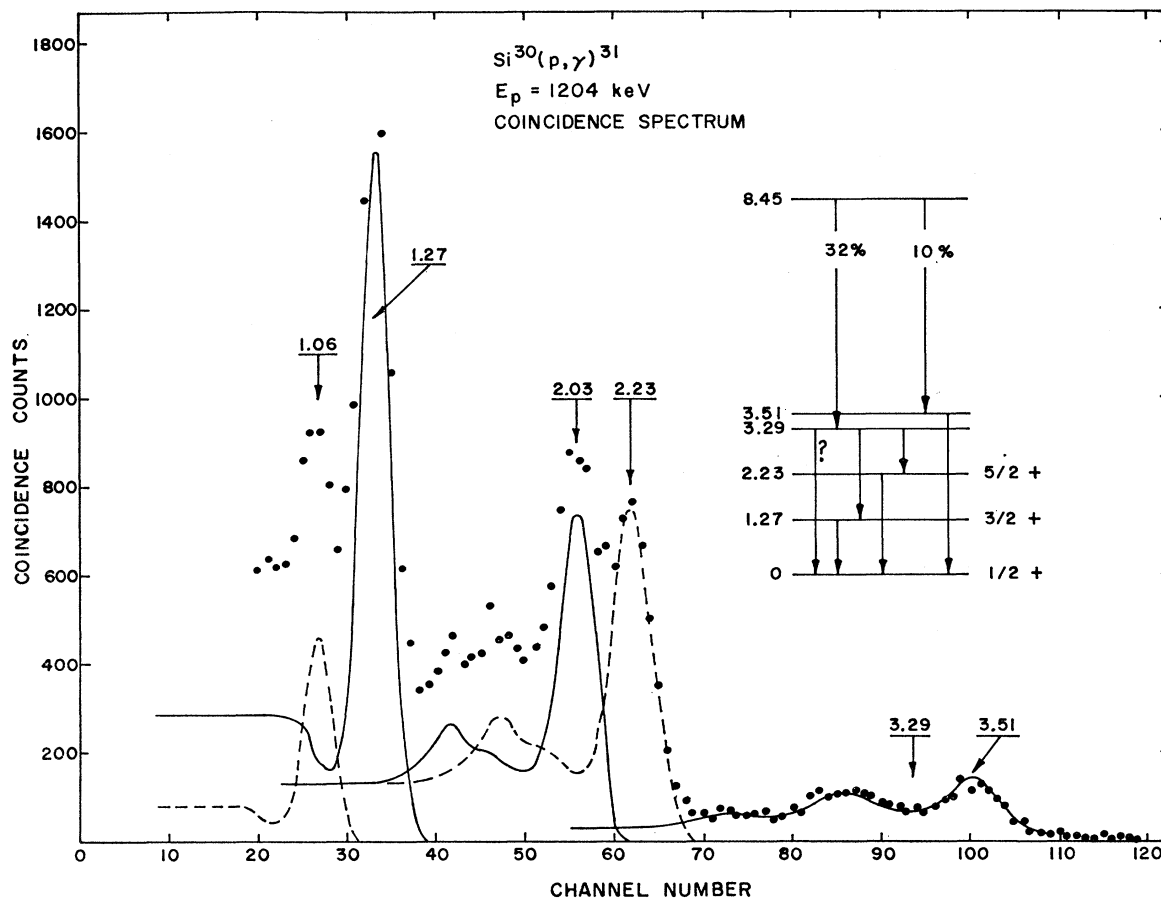


FIG. 2. Spectrum taken in coincidence with 5.16-MeV gamma rays corresponding to the  $r \rightarrow 3.29$  transition at the  $E_p=1204$ -keV resonance. The 3.51-MeV gamma ray is from the  $r \rightarrow 3.51 \rightarrow 0$  cascade, and part of the intensity of the 2.23-MeV gamma ray is due to the  $r \rightarrow 2.23 \rightarrow 0$  cascade.

the curves of Stanford and Rivers.<sup>21</sup> Finally it should be noted that the phase convention of Eq. (3) is such that the sign of  $\delta_2$  [or  $\delta_3$  in Eq. (4)] is opposite that used for secondary radiations in II. This change is necessary to retain consistency of sign between measurements involving different members of a multiple cascade,<sup>22</sup> and is in accordance with recent practice.

## RESULTS

### 3.29-MeV Level

A measurement of the angular distribution of the  $r \rightarrow 3.29$  transition from the  $\frac{5}{2}^+$ ,  $E_p=760$ -keV resonance in  $\text{Si}^{30}(p,\gamma)\text{P}^{31}$  by Hoogenboom<sup>2</sup> was consistent with a spin assignment of either  $J(3.29)=\frac{3}{2}$  or  $\frac{5}{2}$ . The multipolarity mixing ratio required to fit  $\frac{3}{2}$  was small, whereas that required for  $\frac{5}{2}$  was quite large. Therefore, the assignment  $J(3.29)=\frac{3}{2}$  was concluded to be most

probable. On the other hand, a measurement of the angular distribution of the  $r \rightarrow 3.29$  transition at the  $\frac{5}{2}^+$ ,  $E_p=840$ -keV resonance by Broude, Green, and Willmott<sup>3</sup> led to the conclusion that the 3.29-MeV level is  $\frac{5}{2}^+$ . The decay properties of the 3.29-MeV level reported by these authors are not in agreement. The measurements of Hoogenboom led to the conclusion that the 3.29-MeV level decays primarily (>85%) to the 1.27-MeV level with the  $3.29 \rightarrow 0$  and  $3.29 \rightarrow 2.23$  transitions being weaker than 10 and 5%, respectively. Decay-scheme measurements by Broude *et al.*, at six resonances indicate that the  $3.29 \rightarrow 1.27$  and  $3.29 \rightarrow 2.23$  transitions occur with equal intensities, with the  $3.29 \rightarrow 0$  transition accounting for about 5 or 10% of the total radiation. (See Fig. 20 for the level scheme of  $\text{P}^{31}$ .)

The angular-correlation measurements reported in II were found to be in agreement with  $J(3.29)=\frac{5}{2}$ ; however, other possibilities were not investigated in that study. From decay-scheme measurements at seven resonances in the region  $E_p=1177$ –1509 keV, an average branching ratio of 10:60:30 for the  $3.29 \rightarrow 0$ ,  $3.29 \rightarrow 1.27$ , and  $3.29 \rightarrow 2.23$  transitions was reported in I.

<sup>21</sup> A. L. Stanford, Jr., and W. K. Rivers, Jr., *Rev. Sci. Instr.* **30**, 719 (1959).

<sup>22</sup> G. I. Harris, in *Proceedings of the Conference on the Structure of Low-Medium Mass Nuclei*, edited by L. W. Seagondollar, University of Kansas, 1964 (unpublished).

The value  $\delta = -0.52 \pm 0.05$  (allowing for the different phase convention) for the  $3.29 \rightarrow 1.27$  transition based on angular-distribution measurements at the  $E_p = 1204$ , 1392-, and 1489-keV resonances, and the assumption  $J(3.29) = \frac{5}{2}$ , was reported in II. In the present work, more extensive and accurate angular-correlation and spectral measurements were made in order to confirm  $J(3.29)$ , to better determine the decay scheme, and to obtain  $\delta$  values for both the  $3.29 \rightarrow 1.27$  and  $3.29 \rightarrow 2.23$  transitions.

### Decay Scheme

The resonance at  $E_p = 1204$  keV was found in earlier work (I) to decay 32% of the time via a 5.16-MeV transition to the 3.29-MeV level. Figure 2 shows the pertinent features of the resonance decay scheme along with a spectrum taken in coincidence with pulses from the photopeak of the 5.16-MeV gamma ray. This spectrum is the sum of 20 triple-correlation spectra obtained during a 20-h run with a fixed 8-in.  $\times$  8-in. detector and a movable 5-in.  $\times$  5-in. detector which observed the spectrum shown. The front faces of the large and small detectors were located 11.5 and 7.25 in., respectively, from the target. The component, single gamma-ray lines which make up the observed spectrum are shown. The presence of the 2.03-MeV,  $3.29 \rightarrow 1.27$ , and the 1.06-MeV,  $3.29 \rightarrow 2.23$  transitions is clear. The 3.51-MeV gamma-ray is due to the  $r \rightarrow 3.51 \rightarrow 0$  cascade which accounts for about 10% of the radiation from the resonance. The photopeak position of a possible  $3.29 \rightarrow 0$  transition is indicated in the figure. The solid line through those points in the spectrum corresponding to the 3.51-MeV gamma-ray is a careful reproduction of the shape of a 3.51-MeV calibration curve obtained with the same experimental setup the previous day. It can be seen that the intensity of a  $3.29 \rightarrow 0$  transition, if present, is very weak. The relative intensities of the transitions from the 3.29-MeV level to the ground-, first-, and second-excited states are computed from these data to be  $0.8 \pm 1.2\%$ ,  $77 \pm 2\%$ , and  $23 \pm 2\%$ , respectively. The values given have been corrected for the effects of detector efficiency and the angular correlations which are discussed below. The 2% errors arise mainly from the influence of an estimated 10% uncertainty in the determination of the true intensity of the 1.06-MeV gamma-ray from the spectrum. The uncertainty given for the intensity of the  $3.29 \rightarrow 0$  transition is purely statistical. The allowance of a possible uncertainty of two standard deviations gives an upper limit of about 3% for the  $3.29 \rightarrow 0$  intensity. These values are in excellent agreement with the ratio 75:25 reported earlier<sup>9,22</sup> as a result of spectral measurements at the  $E_p = 2187$  keV resonance. The origin of an observable 3.29-MeV peak in earlier work is felt to be due to an insufficient correction for sum effects. The relatively large distance of the detectors from the target in the present work makes such effects quite small in comparison to those in earlier studies.

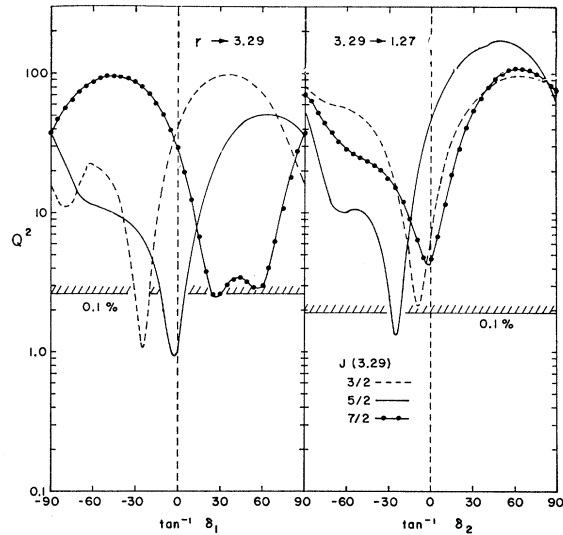


Fig. 3. Projection plots of the  $Q^2$  surfaces for angular-correlation data on the  $r \rightarrow 3.29 \rightarrow 1.27$  and  $3.29 \rightarrow 1.27 \rightarrow 0$  cascades at the  $E_p = 1204$ -keV resonance for various spins of the 3.29-MeV level. Projections in the  $Q^2, \delta_2$  plane are obtained for both cascades. The  $Q^2$  versus  $\delta_2$  curves shown are the results of folding those for the two cascades and using the value  $\delta = 0.28$  for the  $1.27 \rightarrow 0$  transition. The values used for the substate populations of the 3.29-MeV level in the analysis of the latter cascade were computed using the  $\delta_1$  obtained from the  $r \rightarrow 3.29 \rightarrow 1.27$  cascade. The 0.1% statistical confidence "limits" are shown.

The absence of an observable  $3.29 \rightarrow 2.23$  transition in the work of Hoogenboom is not understood; however, it may be due to the influence of very strong correlations of the 1.06-MeV gamma ray which have been observed in the present study.

### Angular Correlations

Angular-correlation measurements, each consisting of several geometries, were performed on the  $r \rightarrow 3.29 \rightarrow 1.27$ ,  $r \rightarrow 3.29 \rightarrow 2.23$ ,  $3.29 \rightarrow 1.27 \rightarrow 0$ , and  $3.29 \rightarrow 2.23 \rightarrow 0$  cascades at the  $E_p = 1204$  keV resonance. A spin of  $\frac{5}{2}$  for this resonance is well established.<sup>5,6,23</sup> The triple cascade from the resonance to the ground state through the 3.29- and 1.27-MeV levels will be discussed first. The following angular correlations were measured:

Cascade	Geometries
(A) $r \rightarrow 3.29 \rightarrow 1.27$	AD1; AD2; (90,V,180); (90,V,90)
(B) $3.29 \rightarrow 1.27 \rightarrow 0$	AD1; (V,90,180); (90,V,180); (90,V,90); (V,90,90)

The results obtained were analyzed for the assumptions  $J(3.29) = \frac{1}{2}, \frac{3}{2}, \frac{5}{2}$ , and  $\frac{7}{2}$  using the known resonance, first-excited state, and ground-state spins.  $J > \frac{7}{2}$  is considered improbable in view of the decay properties. The projection plots of the  $Q^2$  surfaces are shown in Fig. 3 for various spins, and the computer normalized data are shown in Fig. 4. The solid lines in Fig. 4 are

<sup>23</sup> A. K. Val'ter, S. P. Tsytko, Yu. P. Antuf'ev, E. G. Kopanets, and A. N. L'vov, *Izv. Akad. Nauk SSSR, Ser. Fiz.* **25**, 862 (1961).

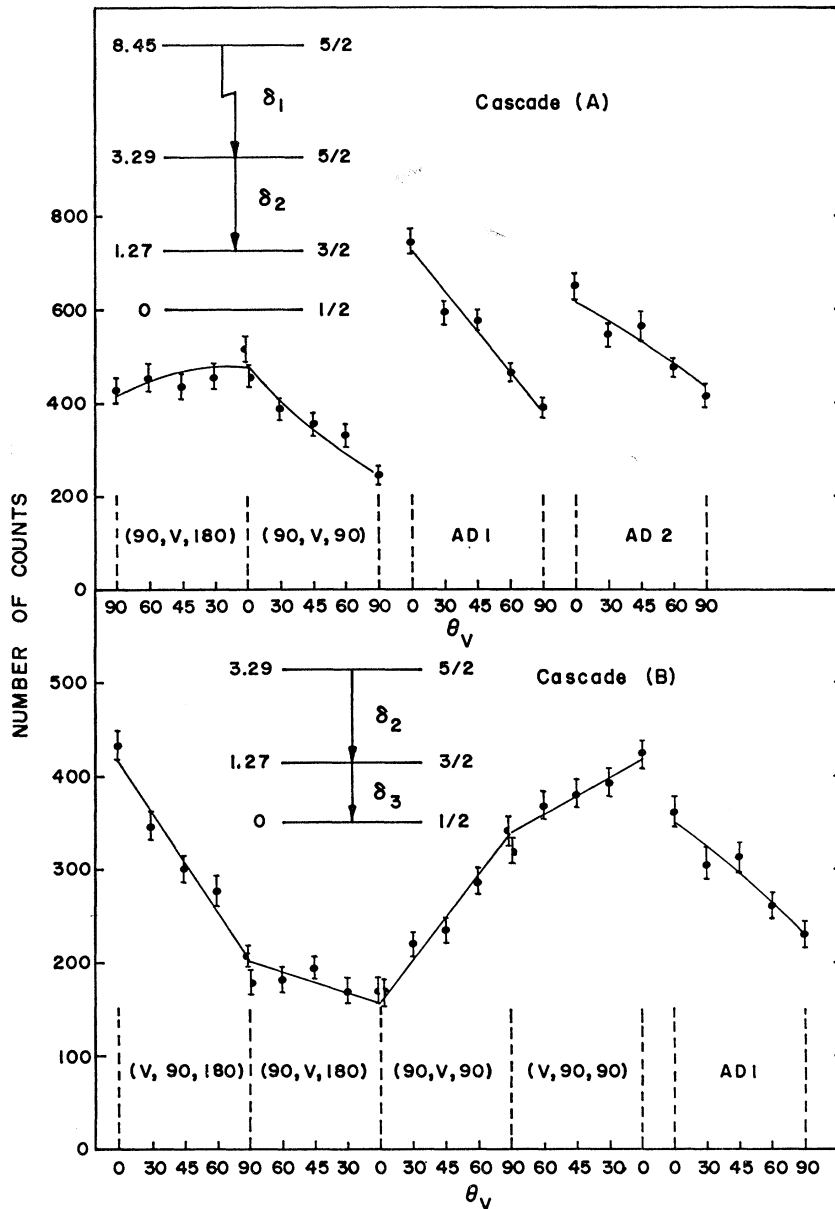


FIG. 4. Angular-correlation data for the  $\gamma \rightarrow 3.29 \rightarrow 1.27 \rightarrow 0$  cascade from the  $E_p = 1204$  keV resonance. The angular distributions and triple-correlation geometries are mutually normalized by the search program. The curves are the best least-square fits for  $J(3.29) = \frac{5}{2}$ .

best least-squares fitted curves computed by the program at the minimum ( $\chi^2$ ) of the  $Q^2$  surface for  $J(3.29) = \frac{5}{2}$ .

From the values of  $\delta_1$  at the minima of the  $Q^2$  projections, the population parameters of the 3.29-MeV level were computed for the various choices of spin. These values of  $P(m)$  were then used in the program for computation of the projections for the  $3.29 \rightarrow 1.27 \rightarrow 0$  cascade. The projections of  $Q^2$  in the  $\delta_2$  plane shown in Fig. 3 are actually composites formed by folding the  $\delta_2$  plane projections of the  $Q^2$  surfaces of both cascades (A) and (B). The folded  $Q^2$  curves were obtained according to the relation<sup>16</sup>

$$Q_F^2 = (N_1 Q_1^2 + N_2 Q_2^2) / (N_1 + N_2), \quad (10)$$

where  $N_1$  and  $N_2$  are the number of degrees of freedom associated with each of the two curves being folded. The effect due to experimental errors in  $\delta_1$  on the  $P(m)$  values of the 3.29-MeV level, and hence on the  $Q^2$  surfaces for cascade (B), was investigated and found to be entirely negligible. For the curves shown,  $\delta_{1.27 \rightarrow 0}$  has been fixed at its known value<sup>5,6</sup> of 0.28. The analysis was also done with  $\delta_{1.27 \rightarrow 0}$  as a free parameter with no significant effect on the conclusions.

It can be seen by inspection of Fig. 3 that the  $J(3.29) = \frac{7}{2}$  assumption leads to unacceptable values of  $Q^2$  for any choice of  $\delta_2$ . Both  $\frac{3}{2}$  and  $\frac{5}{2}$  lead to acceptable minima in  $Q^2$  for some choice of  $\delta_1$ . However, for  $J = \frac{3}{2}$  the minimum value of  $Q^2$  is above the 0.1% confidence

“limit” in the  $Q^2$ ,  $\delta_2$  plane. The minimum value of  $Q^2$  obtained for the choice  $J(3.29)=\frac{1}{2}$  (not shown) was 11.6. The only spin for which acceptable minima are obtained for each mixing ratio is  $J(3.29)=\frac{5}{2}$ . The value of  $\delta_2$  corresponding to this assignment is  $-0.44\pm 0.02$ .

The following angular correlations were measured on the triple cascade from the resonance to the ground state through the 3.29- and 2.23-MeV levels:

Cascade	Geometries
(A) $r \rightarrow 3.29 \rightarrow 2.23$	AD1; (90, V, 180); (90, V, 90)
(B) $3.29 \rightarrow 2.23 \rightarrow 0$	(V, 90, 180); (90, V, 180); (V, 90, 90); (V, 135, 180)

The results of analysis based upon the assumptions  $J(3.29)=\frac{3}{2}$  and  $\frac{5}{2}$  using the known spins of the remaining levels involved are shown in Fig. 5. The data are shown in Fig. 6. The curves drawn through the data points are the computed curves at the minimum of the  $Q^2$  surface for  $J(3.29)=\frac{5}{2}$ . The results in Figs. 5 and 6 involve the assumption that the  $2.23 \rightarrow 0$  transition is pure quadrupole. The effect of interfering octupole radiation was investigated, but the fits to the data were not significantly improved. The “projection” of the  $Q^2$  surface in the  $\delta_2$  plane is a composite of those from cascades (A) and (B) similar to the case discussed above. Again, the error in the value of  $\delta_1$  was found to have an insignificant effect on the analysis of cascade (B).

By inspection of Fig. 5, it can be seen that an acceptable value of  $Q^2$  is obtained only for  $J(3.29)=\frac{5}{2}$ . The value of  $\delta$  for the  $3.29 \rightarrow 2.23$  transition corresponding to this assignment is  $\delta_2 = -0.41 \pm 0.06$ . The average value of  $\delta_{r \rightarrow 3.29}$  is  $-0.02 \pm 0.02$ .

### 3.51-MeV Level

This level is known to decay primarily to the ground state.<sup>2-4</sup> It was shown in I that there also exists a transition to either the 1.27- or 2.23-MeV levels (or both) which accounts for about 40% of the total radiation from the 3.51-MeV level. The relative energies of the 1.27-, 2.23-, and 3.51-MeV levels make it impossible to determine by ordinary coincidence techniques the actual decay scheme of the 3.51-MeV level. It is possible in principle, however, to determine which levels are involved in the decay (and in what proportion) by means of angular-correlation measurements. This particular problem has been discussed earlier<sup>5, 22, 24</sup> along with the analysis of some early angular-correlation measurements which led to the conclusion that the cascade decay of the 3.51-MeV level involves the 1.27-MeV level instead of the 2.23-MeV level. In later attempts at more rigorous analysis of these data, it was found that the data were not self-consistent unless it was assumed both levels were involved. In the following, we present the results and analysis of new measurements, made under improved conditions, which help to clarify this peculiarly complicated problem. First,

<sup>24</sup> G. I. Harris, Bull. Am. Phys. Soc. 8, 321 (1963).

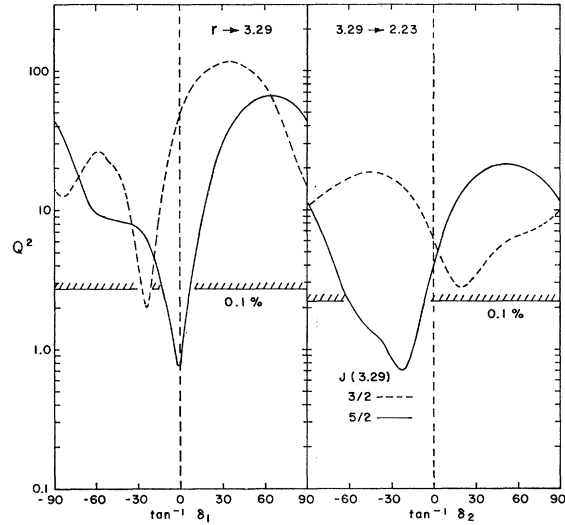


FIG. 5. Projection plots of the  $Q^2$  surfaces for the  $r \rightarrow 3.29 \rightarrow 2.23 \rightarrow 0$  cascade from the  $E_p=1204$  keV resonance for the assumptions  $J=3/2$  and  $5/2$  for the 3.29 MeV level. The  $Q^2$  versus  $\delta_2$  curves shown result from folding those for the  $r \rightarrow 3.29 \rightarrow 2.23$  and  $3.29 \rightarrow 2.23 \rightarrow 0$  measurements and using pure quadrupole radiation for the  $2.23 \rightarrow 0$  transition.

however, we present the results of angular-correlation measurements performed to verify the spin of the 3.51-MeV level.

### Spin of the 3.51-MeV Level

The results of angular-correlation measurements on the  $r \rightarrow 3.51 \rightarrow 0$  cascade at the  $E_p=1322$  keV resonance and the analysis are shown in Figs. 7 and 8. The spin of the 1322-keV resonance is known to be  $\frac{5}{2}$  from earlier work.<sup>5, 6, 23</sup> In addition, measurements of geometries (90, V, 180), (90, V, 90), AD1, and AD2 were performed on the corresponding, but weaker, cascade at the 1204-keV resonance. These data are not shown but the results are given below. The results of the analysis of the 1322-keV data for  $J(3.51)=\frac{3}{2}$ ,  $\frac{5}{2}$ , and  $\frac{7}{2}$  are shown in Fig. 7. It is clear that an acceptable solution is obtained only for  $\frac{3}{2}$ . The possibility that  $J(3.51)=\frac{1}{2}$  was also investigated, but an acceptable fit was not obtained ( $\chi^2=7.7$ ). The values of  $\delta$  for the  $3.51 \rightarrow 0$  transition obtained from these data are  $-0.43 \pm 0.03$  or  $8.1_{-1.2}^{+1.9}$ . The values obtained from the data at the 1204-keV resonance are  $-0.39 \pm 0.04$  or  $6.3_{-0.9}^{+1.3}$ . The adopted average values are  $-0.41 \pm 0.03$  or  $7.1 \pm 1.0$ . In comparison, the values reported by Hoogenboom<sup>2</sup> are  $-0.34 \pm 0.05$  or  $7 \pm 3$ .

### Decay Scheme

In order to verify the existence of transitions from the 3.51-MeV level to levels other than the ground state, a spectrum at the 1322-keV resonance was recorded by the 8-in.  $\times$  8-in. detector at  $\theta_2=90^\circ$  in coincidence with the photopeak of the  $r \rightarrow 3.51$  transition

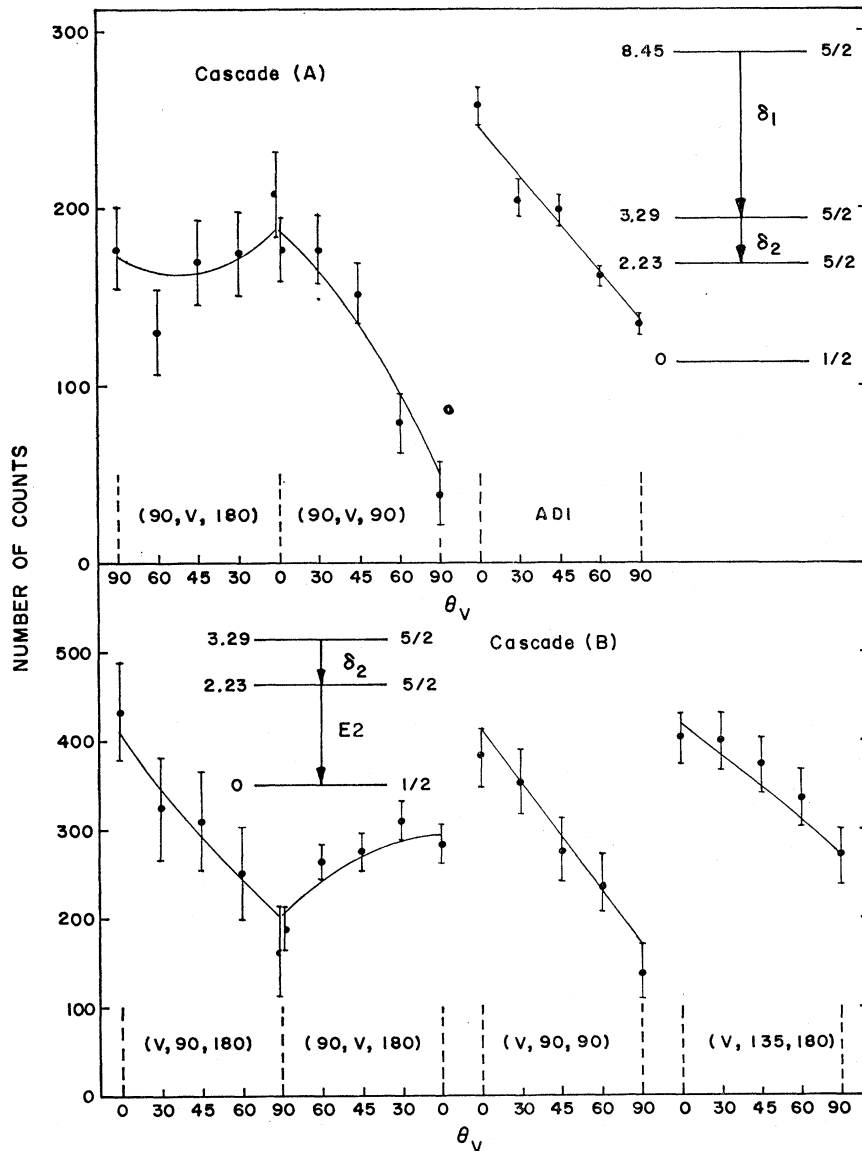


FIG. 6. Angular-correlation data for the  $r \rightarrow 3.29 \rightarrow 2.23 \rightarrow 0$  transition from the  $E_p = 1204$  keV resonance. The curves are the best least-square fits for  $J(3.29) = \frac{5}{2}$ .

observed by a 5-in.  $\times$  5-in. detector at  $\theta_1 = 90^\circ$  ( $\phi = 180^\circ$ ). An additional spectrum was simultaneously recorded in coincidence with pulses from a window of equal width set just above the photopeak of the  $r \rightarrow 3.51$  transition. This spectrum was subtracted from the first to compensate for effects of higher energy transitions in the spectrum. The resultant gamma-ray lines are shown in Fig. 9 where the component gamma-ray lines are shown. The component labeled 2.03 MeV is probably due to a weak primary transition to the 3.29-MeV level which would appear in the window set over the  $r \rightarrow 3.51$  photopeak and not be completely compensated by the higher energy window. The components at 1.27 and 2.23 MeV must be due to transitions to the 1.27- and/or 2.23-MeV

levels from the 3.51-MeV level. The intensities of the 3.51-, 2.23-, and 1.27-MeV peaks, after correction for angular correlations, are 2590, 1450, and 1600 counts, respectively. From this, we conclude that the relative intensity of the  $3.51 \rightarrow 0$  transition is  $64 \pm 3\%$  which agrees well with the value 60% reported earlier.<sup>4</sup>

A series of triple-correlation measurements were performed to determine, for the remaining 36% of the radiation from the 3.51-MeV level, the intensity ratio  $R = (3.51 \rightarrow 1.27)/(3.51 \rightarrow 2.23)$  and the dipole-quadrupole mixing ratios for each of these transitions. Both the 1.27- and 2.23-MeV levels decay only to the ground state; and the known pure  $E2$  character for the  $2.23 \rightarrow 0$  transition and the value  $\delta = 0.28$  for the  $1.27 \rightarrow 0$  transi-

tion are assumed in the analysis.<sup>5,6</sup> The triple correlations are referred to as follows:

- (a) [5.06(90°), 1.27(V),  $\phi=180^\circ$ ],
- (b) [5.06(90°), 1.27(V),  $\phi=90^\circ$  ],
- (c) [5.06(90°), 2.23(V),  $\phi=180^\circ$ ],
- (d) [5.06(90°), 2.23(V),  $\phi=90^\circ$  ],
- (e) [1.27(90°), 2.23(V),  $\phi=180^\circ$ ],
- (f) [2.23(90°), 1.27(V),  $\phi=180^\circ$ ],
- (g) [2.23(90°), 1.27(V),  $\phi=90^\circ$  ],
- (h) [1.27(90°), 2.23(V),  $\phi=90^\circ$  ],

where, for example, correlation (a) means that the intensity of the 1.27-MeV peak was observed in the movable detector in coincidence with the 5.06-MeV gamma ray observed in a detector fixed at  $\theta=90^\circ$ ,  $\phi=180^\circ$ . This special notation is used because the 1.27- and 2.23-MeV peaks in the coincidence spectra are assumed to each arise from two transitions (see Fig. 9). The standard notations thus do not apply. Correlation (a), in our previous notation, is a combination of the geometries (90, V, 180) and (90, u, V, 180), weighted by the branching ratio R, for the  $r \rightarrow 3.51 \rightarrow 2.23$  and  $r \rightarrow 3.51 \rightarrow 1.27 \rightarrow 0$  cascades, respectively. Similarly, correlation (e) is a combination, weighted by R, of geometries (V, 90, 180) and (90, V, 180) for the  $3.51 \rightarrow 1.27 \rightarrow 0$  and  $3.51 \rightarrow 2.23 \rightarrow 0$  cascades, respectively.

The measurements discussed above on the  $r \rightarrow 3.51 \rightarrow 0$  cascade yield for the  $r \rightarrow 3.51$  transition a

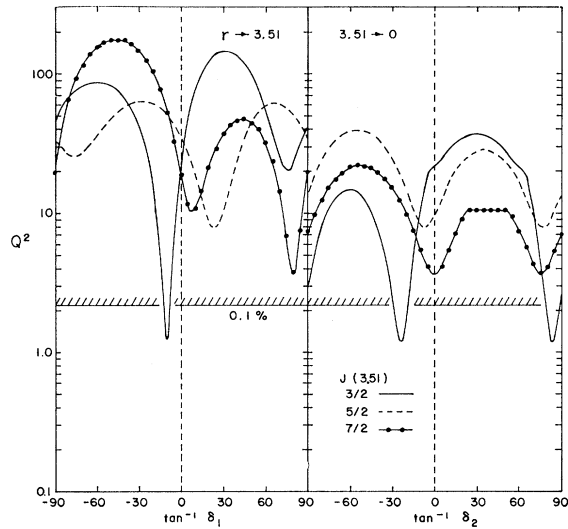
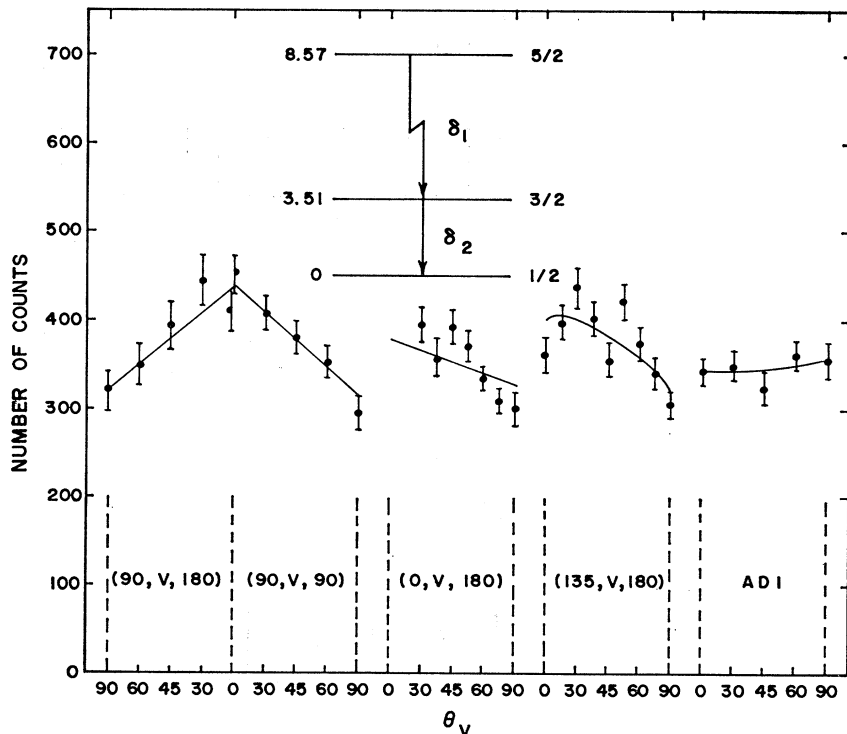


FIG. 7. Projection plots of the  $Q^2$  surface for the  $r \rightarrow 3.51 \rightarrow 0$  cascade from the  $E_p=1322$  keV resonance for spins  $J(3.51)=\frac{3}{2}$ ,  $\frac{5}{2}$ , and  $\frac{7}{2}$ .

value  $\delta = -0.18 \pm 0.02$  (see Fig. 7) which was used to compute the populations of the substates of the 3.51-MeV level required in the analysis of correlations (e)  $\rightarrow$  (h). As a first step in the analysis, correlations (a)  $\rightarrow$  (d) plus the angular distribution (AD1) of the  $r \rightarrow 3.51$  transition were treated using the "single-parameter method" of Ref. 15. {In this method, the  $P(m)$  and  $H_M$  of Eq.(1) are combined into a single

FIG. 8. Angular-correlation data for the  $r \rightarrow 3.51 \rightarrow 0$  cascade from the  $E_p=1322$  keV resonance. The curves are the best fits for  $J(3.51) = \frac{3}{2}$ .



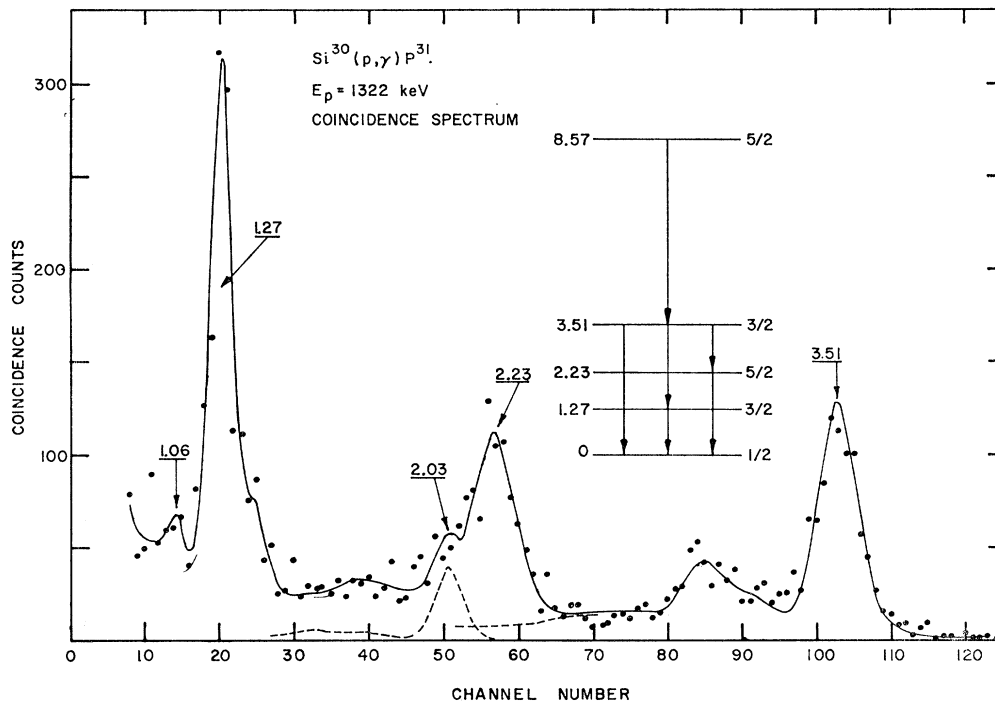


FIG. 9. Spectrum taken in coincidence with 5.06-MeV gamma rays corresponding to the  $r \rightarrow 3.51$  transition at the  $E_p = 1322$  keV resonance. The relevant decay scheme is shown.

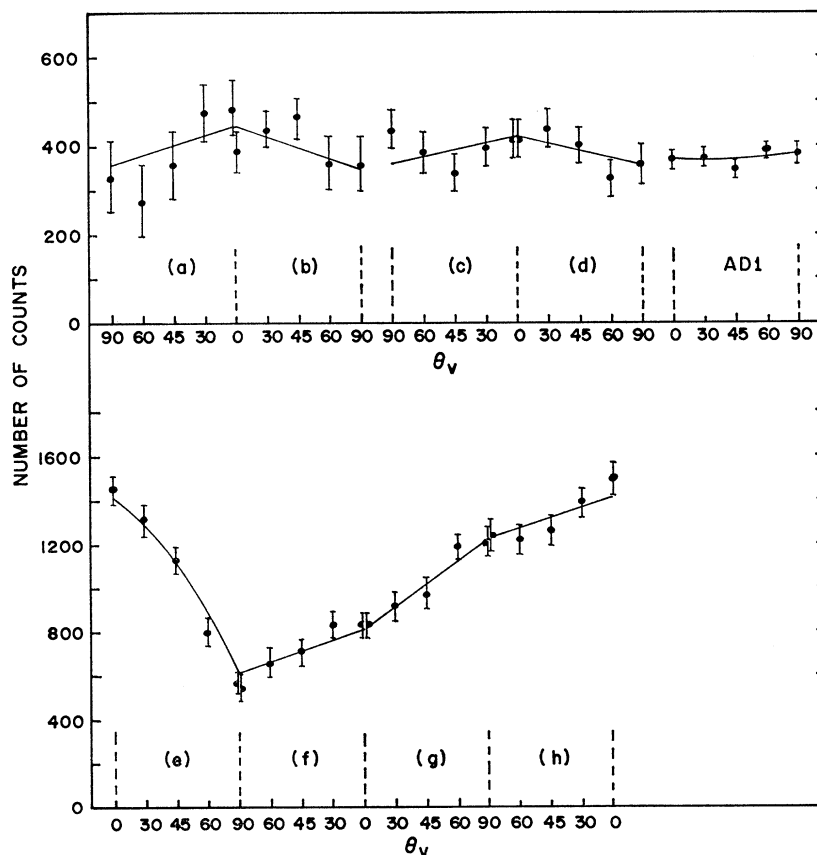


FIG. 10. Angular-correlation data for the combined cascades  $r \rightarrow 3.51 \rightarrow 1.27 \rightarrow 0$  and  $r \rightarrow 3.51 \rightarrow 2.23 \rightarrow 0$  from the  $E_p = 1322$  keV resonance. The experimental conditions for the correlations (a) through (h) are explained in the text. AD1 refers to the angular distribution of the  $r \rightarrow 3.51$  transition. The results for correlations (a) through (h) were corrected for the effects of tails of higher energy transitions by subtracting spectra from coincidence windows set above the windows which include the photopeaks of the gamma rays under consideration. The curves represent the best fit to the data at the solution.

element  $I_{mM}$ . The elements of the  $[I_{mM}]$  matrix are then determined by least-squares solution of Eq. (1) with  $\delta_1$  treated as a parameter.} In the present case  $I_{mM} = H_M$  since  $P(\frac{1}{2}) = 1$  and  $P(m > \frac{1}{2}) = 0$ . We note however that the  $H_M$  of this problem are specific combinations of the  $H_M$  for the two transitions to which the 1.27- (or 2.23-) MeV gamma rays correspond. If we denote the combination by  $\mathcal{H}_M$ , then we have for correlations (a) and (b),

$$\mathcal{H}_M^{a,b} = H_M(\frac{3}{2}, \frac{5}{2}, \delta_1) + R u_M(\frac{3}{2}, \frac{3}{2}, \delta_2) H_M(\frac{3}{2}, \frac{1}{2}, \delta_3), \quad (11)$$

and for correlations (c) and (d),

$$\mathcal{H}_M^{c,d} = u_M(\frac{3}{2}, \frac{5}{2}, \delta_1) H_M(\frac{5}{2}, \frac{1}{2}, \delta_4) + R H_M(\frac{3}{2}, \frac{3}{2}, \delta_2), \quad (12)$$

where  $\delta_1$  and  $\delta_2$  are the mixing ratios for the  $3.51 \rightarrow 2.23$  and  $3.51 \rightarrow 1.27$  transitions, respectively. The mixing ratios  $\delta_3$  and  $\delta_4$  for the  $1.27 \rightarrow 0$  and  $2.23 \rightarrow 0$  transitions are treated as known quantities. The unknown quantities are thus  $\delta_1$ ,  $\delta_2$ , and  $R$ . [Note that the spin of the 3.51-MeV level allows only  $M=0, 2$  in correlations (a)  $\rightarrow$  (d).]

Ratios having the same formal dependence upon  $\delta_1$ ,  $\delta_2$ , and  $R$  as do  $\mathcal{H}_M/\mathcal{H}_0$  were obtained from correlations (e)  $\rightarrow$  (h) by determining from the data by least-squares analysis the coefficients in the expression

$$W_i = \sum_k (A_k/A_0)_i P_k(\cos\theta),$$

where  $i$  refers to the correlations (e)  $\rightarrow$  (h). The  $(A_k)_i$  can be expressed in terms of  $\delta_1$ ,  $\delta_2$ , and  $R$  in a form similar to Eqs. (11) and (12). A total of seven ratios were thereby determined from the data shown in Fig. 10. The seven corresponding equations are written as

$$(\mathcal{A}_j \pm \Delta \mathcal{A}_j) = F_j(\delta_1, \delta_2, R), \quad j=1, \dots, 7, \quad (13)$$

where  $\mathcal{A}_j$  is used to denote the experimental ratios. For fixed values  $\bar{R}$  of the branching ratio between  $R=0$  and  $R=\infty$ , the value of  $Q^2$ , where

$$Q^2 = \frac{1}{N} \sum_j \left( \frac{1}{\Delta \mathcal{A}_j} \right)^2 [F_j(\delta_1, \delta_2, \bar{R}) - \mathcal{A}_j]^2, \quad (14)$$

was computed by a special program<sup>25</sup> at grid points with  $5^\circ$  spacing in the variables  $\tan^{-1}\delta_1$  and  $\tan^{-1}\delta_2$ . The value  $N=5$  was used for the number of degrees of freedom. For each fixed value of  $R$ , the minimum value of  $Q^2$ ,  $Q^2_{\min}(\bar{R})$ , was selected from the grid and plotted versus  $\tan^{-1}(R)^{1/2}$  as shown in Fig. 11. (The  $Q^2$  minima occurred at unique values of  $\delta_1$  and  $\delta_2$  in each grid.) The minimum point in the  $Q^2_{\min}$  curve is referred to as  $\chi^2(R_s)$ , where  $R_s$  is the best least-squares value of the branching ratio. The range of  $R$  corresponding to one "standard deviation" is obtained by determining the values of  $R$  which correspond to  $Q^2_{\min} = [(N+1)/N]\chi^2(R_s)$ . This range is shown in Fig. 11. Also shown in Fig. 11 are the projections of the  $Q^2$

<sup>25</sup> The program for this computation was written by A. K. Hyder of this laboratory.

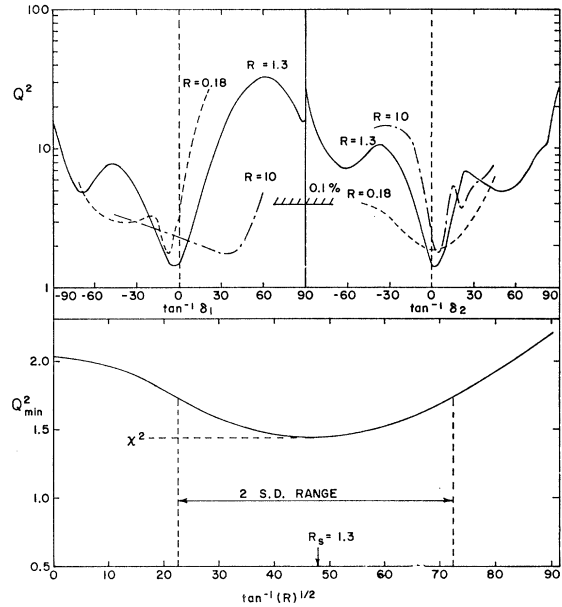


FIG. 11. Results of analysis of the data in Fig. 10 for the determination of the intensity ratio  $R = (3.51 \rightarrow 1.27)/(3.51 \rightarrow 2.23)$  and the value of the dipole-quadrupole mixing ratios of these transitions. The ratios  $\delta_1$  and  $\delta_2$  refer to the  $3.51 \rightarrow 2.23$  and  $3.51 \rightarrow 1.27$  transitions, respectively. The upper two diagrams are projection plots of the  $Q^2$  surface in the  $\delta_1$  and  $\delta_2$  planes. The lower curve shows the dependence on  $R$  of the minimum of the  $Q^2$  surface.  $Q^2$  and  $Q^2_{\min}$  are defined in the text.

surfaces in the  $Q^2$ ,  $\delta_1$  and  $Q^2$ ,  $\delta_2$  planes for  $R=R_s$  and at the one-standard-deviation points. The "best" values  $R_s = 1.3_{-1.1}^{+8.7}$ ,  $\delta_1 = -0.05_{-0.11}^{+1.05}$ , and  $\delta_2 = 0.06 \pm 0.19$  are obtained from this diagram. The experimental error of the branching ratio is seen to be rather large; however, the multipolarity mixing ratios are not very sensitive to  $R$  and are better determined. These values are in general agreement with tentative results reported earlier.<sup>22</sup> From the definition of  $R_s$  and the results above, we conclude that the 3.51-MeV level decays with relative intensities  $64 \pm 3\%$ ,  $20 \pm 14\%$ , and  $16 \pm 14\%$ , to the ground state, 1.27-MeV level, and 2.23-MeV level, respectively.

#### 4.26-MeV Level

This level was reported in I to decay with the intensity ratio 84:16 to the ground and first-excited states, and a spin of  $\frac{3}{2}$  was reported in II. These conclusions were derived from an analysis of the gamma-ray (singles) spectrum and angular-distribution measurements at the  $E_p = 1204$ -keV resonance. It was shown in I that this resonance decays with relative intensity 24% to the 4.26-MeV level. This result has been confirmed by Van Rinsvelt and Smith who report a relative intensity of 25%.<sup>6</sup> However, they did not discuss the decay properties or the spin of the 4.26-MeV level.

The 1204-keV resonance corresponds to a  $P^{31}$  excitation energy of 8.45 MeV. The  $r \rightarrow 4.26$  and  $4.26 \rightarrow 0$  transitions are thus unresolved in the spectra. This

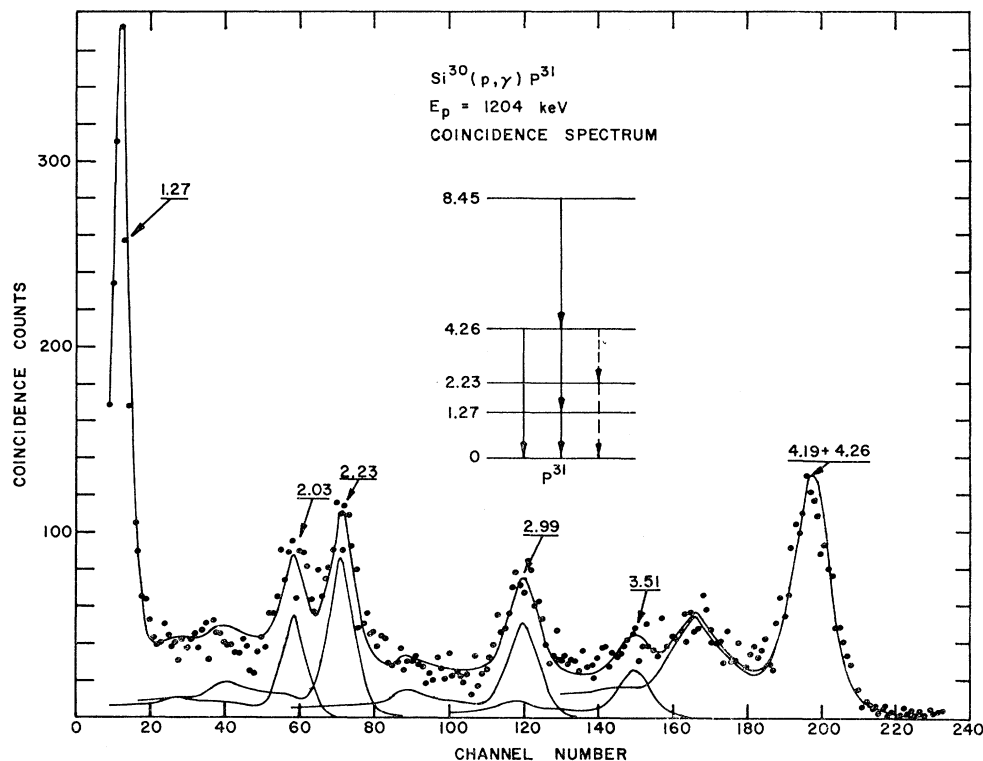


FIG. 12. Spectrum in coincidence with the photopeak of the unresolved 4.19- and 4.26-MeV gamma rays which correspond to the  $r \rightarrow 4.26 \rightarrow 0$  cascade at the  $E_p = 1204$  keV resonance. The origin of the various components of this spectrum is discussed in the text.

circumstance made it impossible to derive well-defined values for the multipolarity mixings of these two transitions from the angular-distribution measurement reported in II. In what follows, we discuss the results of more extensive coincidence spectra and triple-correlation measurements at the 1204-keV resonance, which more accurately determine decay properties and mixing ratios and which confirm the spin of the 4.26-MeV level. It is found that, although the analysis is made somewhat more inconvenient, the fact that the  $r \rightarrow 4.26$  and  $4.26 \rightarrow 0$  transitions are unresolved leads to no particular difficulty in arriving at a unique spin assignment and good values for branching and mixing ratios.

#### Decay Scheme

Figure 12 shows a spectrum from the 8-in.  $\times$  8-in. detector at  $\theta = 0^\circ$  in coincidence with the photopeak of the 4.2-MeV "gamma ray" observed in a 5-in.  $\times$  5-in. detector at  $\theta = 90^\circ$  at the  $E_p = 1204$ -keV resonance. (A singles spectrum taken with a 5-in.  $\times$  5-in. detector at  $\theta = 55^\circ$  was presented in I.) The 4.2-MeV "gamma ray" is, of course, a combination of the 4.19-MeV,  $r \rightarrow 4.26$  and 4.26-MeV,  $4.26 \rightarrow 0$  transitions. The presence of the 2.23-, 3.51-MeV gamma rays, and most of the intensity of the 1.27- and 2.03-MeV gamma rays, in this coincidence spectrum are due to the fact that the coincidence window necessarily admits pulses from high-energy primary transitions to the 1.27-, 2.23-, 3.29-, and 3.51-MeV levels. Part of the intensity of the

1.27-MeV peak and the 2.99-MeV gamma ray are clearly due to a  $4.26 \rightarrow 1.27 \rightarrow 0$  cascade. The gamma-ray peak at 4.2 MeV is due to a  $r \rightarrow 4.26 \rightarrow 0$  cascade. A possible  $4.26 \rightarrow 2.23$  transition would have very nearly the same energy as the  $3.29 \rightarrow 1.27$  transition which appears.

The observed total intensities of the spectrum components at 2.03, 2.99, and 4.2 MeV are 1220, 1670, and 5800 counts, respectively. After correction for the angular correlations discussed below, and allowing for the unresolved character of the 4.2-MeV peak, the true intensities of the  $4.26 \rightarrow 0$  and  $4.26 \rightarrow 1.27$  transitions are 3670 and 980 counts, respectively. It is found by careful analysis of the width and location of the coincidence window in the 5-in.  $\times$  5-in. singles spectrum that at least 85% of the intensity of the 2.03-MeV peak can be accounted for by a  $3.29 \rightarrow 1.27$  transition. The remaining 15% could be due to a  $4.26 \rightarrow 1.27$  transition. These results lead to the relative intensities  $76 \pm 3$ ,  $20 \pm 3$ , and  $4 \pm 3\%$  for the  $4.26 \rightarrow 0$ ,  $4.26 \rightarrow 1.27$ , and  $4.26 \rightarrow 2.23$  transitions, respectively. For comparison, the results reported in I were 84, 16, and 0% based on a singles spectrum alone.

#### Angular Correlations

The results of angular-distribution and triple-correlation measurements on the  $r \rightarrow 4.26 \rightarrow 0$  and  $r \rightarrow 4.26 \rightarrow 1.27 \rightarrow 0$  cascades at the ( $J = \frac{5}{2}$ ) 1204-keV resonance are shown in Fig. 13. The double cascades

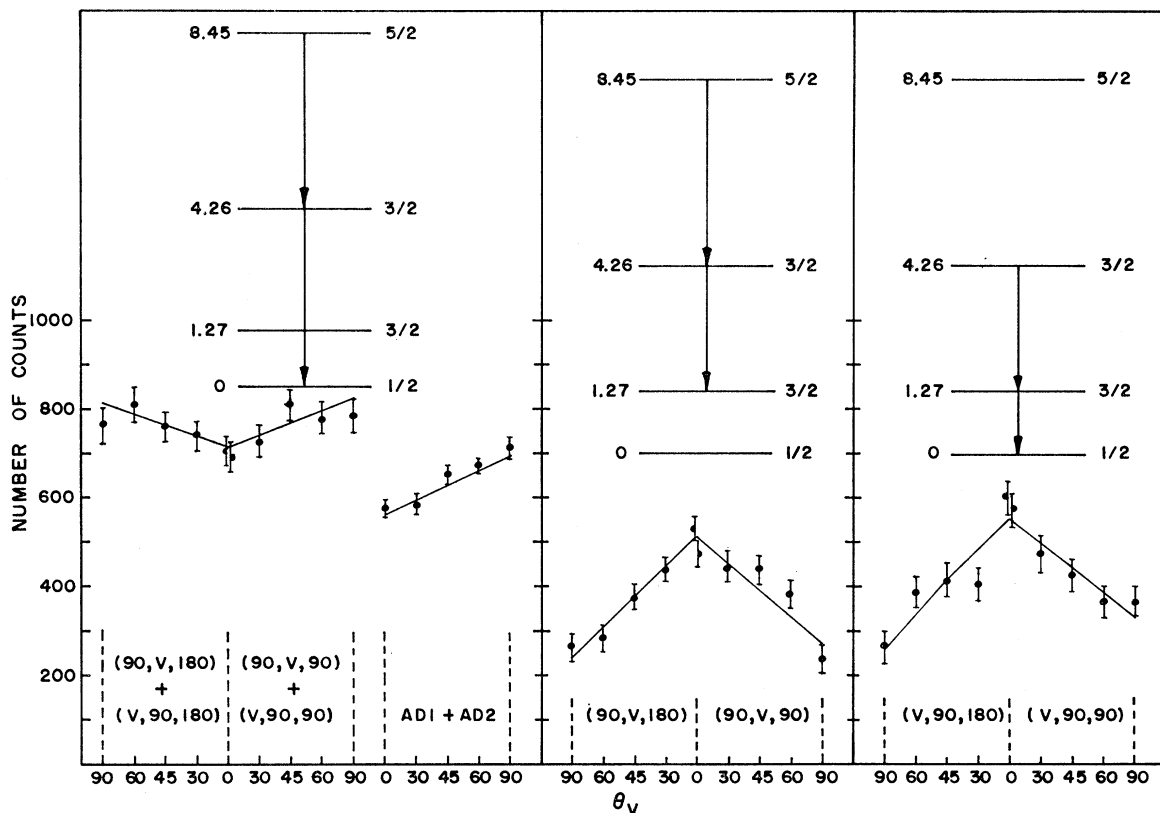


FIG. 13. Angular-correlation data for the  $r \rightarrow 4.26 \rightarrow 0$ ,  $r \rightarrow 4.26 \rightarrow 1.27$ , and  $4.26 \rightarrow 1.27 \rightarrow 0$  cascades at the  $E_p = 1204$  keV resonance. The data for the  $r \rightarrow 4.26 \rightarrow 0$  cascade correspond to the indicated combined geometries. The spectrum from a compensating window set just above the 1.27-MeV transition has been used to correct the data for the  $4.26 \rightarrow 1.27 \rightarrow 0$  cascade. The curves represent the best fit for  $J(4.26) = \frac{3}{2}$ .

which are relevant to each set of measurements are indicated. In order to analyze the data from the unresolved members of the  $r \rightarrow 4.26 \rightarrow 0$  cascade, the computer program was modified so that it would compare the data with the appropriate "combined geometry" theoretical expressions. This modification consisted of replacing the factor  $X_{KM}^N(\theta_1, \theta_2, \phi)$  in Eq. (2) with the sum  $X_{KM}^N(\theta_1, \theta_2, \phi) + X_{KM}^N(\theta_2, \theta_1, \phi)$ . The populations of the 4.26-MeV level, which are used in the analysis of data for the  $4.26 \rightarrow 1.27 \rightarrow 0$  cascade, were computed from Eq. (6) and the value of  $\delta_{r \rightarrow 4.26}$  determined from the analysis of the other two cascades.

The results of the analysis of these data are shown in Fig. 14. The upper two diagrams show the projections of  $Q^2$  surfaces for the  $r \rightarrow 4.26 \rightarrow 0$  cascade for  $J(4.26) = \frac{3}{2}$ ,  $\frac{5}{2}$ , and  $\frac{7}{2}$ . It is clear that, of these choices of spin, only  $\frac{3}{2}$  yields an acceptable value of  $\chi^2$ . The value of  $\chi^2$  for  $J(4.26) = \frac{1}{2}$  (not shown) was 2.97.  $J(4.26) > \frac{7}{2}$  is considered improbable in view of the observed decay properties. Hence  $J(4.26) = \frac{3}{2}$ . For  $J = \frac{3}{2}$ , the values of  $\delta_{r \rightarrow 4.26}$  and  $\delta_{4.26 \rightarrow 0}$  are  $-0.04 \pm 0.04$ , and  $-0.32 \pm 0.04$  or  $4.7 \pm 0.9$ , respectively. The only previously reported values are  $|\delta_{r \rightarrow 4.26}| \leq 0.26$  in II, and the preliminary values  $\delta_{4.26 \rightarrow 0} = -0.32$  or  $4.7$  in Ref. 22.

The lower two diagrams of Fig. 14 show the projections of the  $Q^2$  surface for the  $r \rightarrow 4.26 \rightarrow 1.27 \rightarrow 0$  cascade assuming  $J(4.26) = \frac{3}{2}$ . The projections in the  $Q^2$ ,  $\delta_{4.26 \rightarrow 1.27}$  plane are "folded" projections obtained from the analysis of the  $r \rightarrow 4.26 \rightarrow 1.27$  and  $4.26 \rightarrow 1.27 \rightarrow 0$  cascades in which  $\delta_{1.27 \rightarrow 0}$  has been fixed at 0.28. (The analysis was also conducted with  $\delta_{1.27 \rightarrow 0}$  treated as a parameter. No significant improvement in the fit was obtained.) The values of the two mixing ratios are  $\delta_{r \rightarrow 4.26} = -0.07 \pm 0.07$  and  $\delta_{4.26 \rightarrow 1.27} = -0.25 \pm 0.05$ . The weighted average value of  $\delta_{r \rightarrow 4.26}$  is  $-0.05 \pm 0.04$ .

During the analysis of the triple-correlation data on the  $4.26 \rightarrow 1.27 \rightarrow 0$  cascade at the 1204-keV resonance, the presence of a previously unreported weak cascade through the 4.63-MeV level was discovered. However, a stronger cascade through this level was subsequently discovered at the 1095-keV resonance and is discussed in the following section.

#### $E_p = 1095$ -keV Resonance and the 4.63-MeV Level

The relatively weak resonance at 1095 keV was studied by Van Rinsvelt and Smith<sup>6</sup> who found that

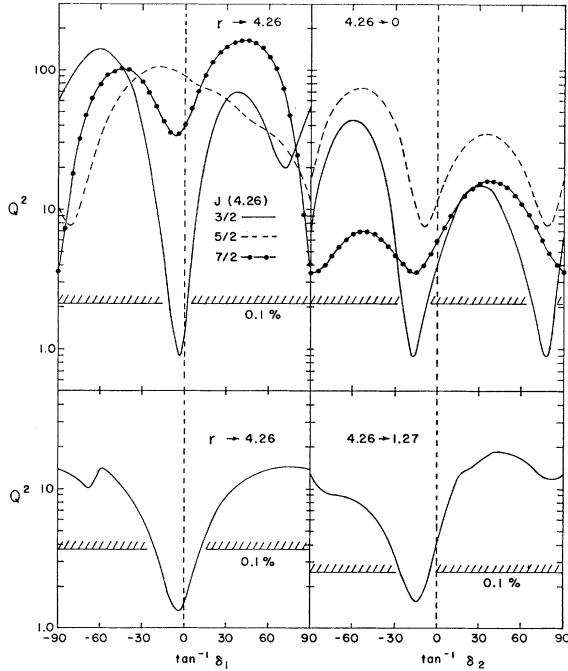


FIG. 14. Projection plots of the  $Q^2$  surfaces for the analysis of the data of Fig. 13. The upper two diagrams are for the  $r \rightarrow 4.26 \rightarrow 0$  cascade, and the lower two are for the  $r \rightarrow 4.26 \rightarrow 1.27 \rightarrow 0$  cascade. The lower, right-hand curves were obtained by folding the projection plots of  $Q^2$  in the  $\delta_{4.26 \rightarrow 1.27}$  plane for the  $r \rightarrow 4.26 \rightarrow 1.27$  and  $4.26 \rightarrow 1.27 \rightarrow 0$  cascades. The value of  $\delta_{1.27 \rightarrow 0}$  has been fixed at 0.28 for these diagrams.

$J_r = \frac{5}{2}$  from angular-correlation measurements on the  $r \rightarrow 1.27 \rightarrow 0$  cascade. They also reported that transitions to the 4.59- and 5.01-MeV levels account for 9

and 15% of the radiation from the resonance. In preliminary measurements at this resonance performed with the intent of determining the spin of the 5.01-MeV level, it was found that coincidence spectra, and singles spectra obtained with the 8-in.  $\times$  8-in. detector, were inconsistent with these reported transitions. It was found, instead, that the observed gamma-ray energies and relative intensities were consistently explained by a (15.3%) transition to the 4.63-MeV level. The following measurements were thus performed to better determine the decay scheme of the resonance and the decay scheme and spin of the 4.63-MeV level.

*Decay Scheme*

Figure 15 shows a singles spectrum obtained at  $E_p = 1095$  keV with the 8-in.  $\times$  8-in. detector located with its axis at  $55^\circ$  relative to the proton beam and its front face 3.25 in. from the target. Background was removed from this spectrum in the following manner: A control circuit was constructed which would switch the multichannel analyzer from its add mode to subtract mode after a predetermined number of analyzer live-time clock pulses, and at the same time shift the proton beam energy to a value off resonance by changing the current in the beam analyzing magnet. The system was set to cycle in this manner several hundred times during the measurement. Very satisfactory removal of background, both from target contaminants and natural radioactivity, has been obtained in other measurements using this method. There is some evidence in the present case, however, that the (relatively strong) 1.46-MeV  $K^{40}$  line was not entirely re-

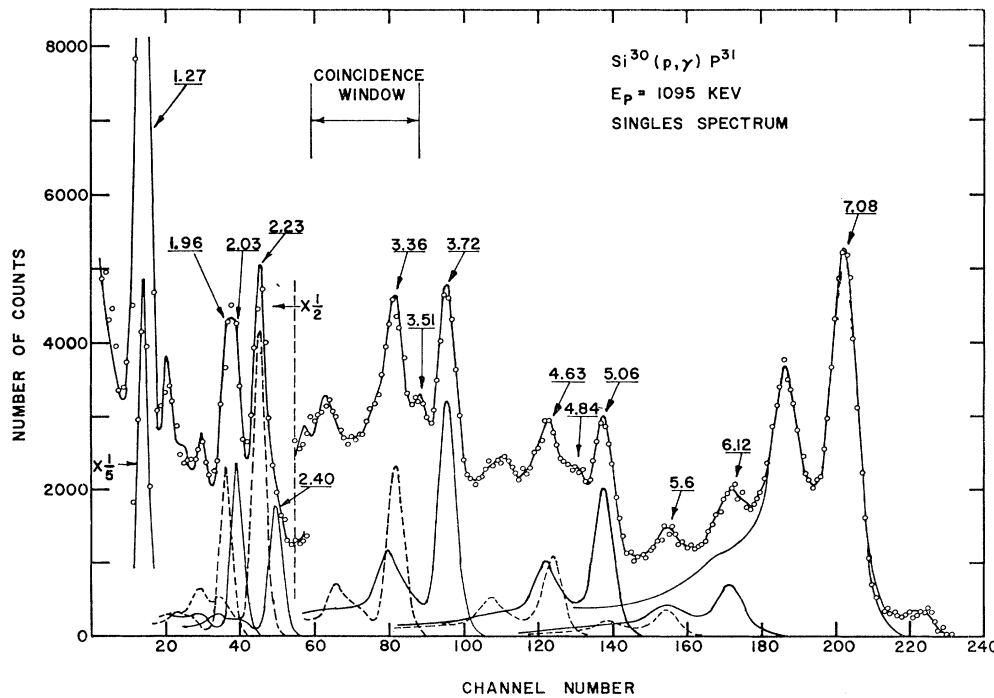
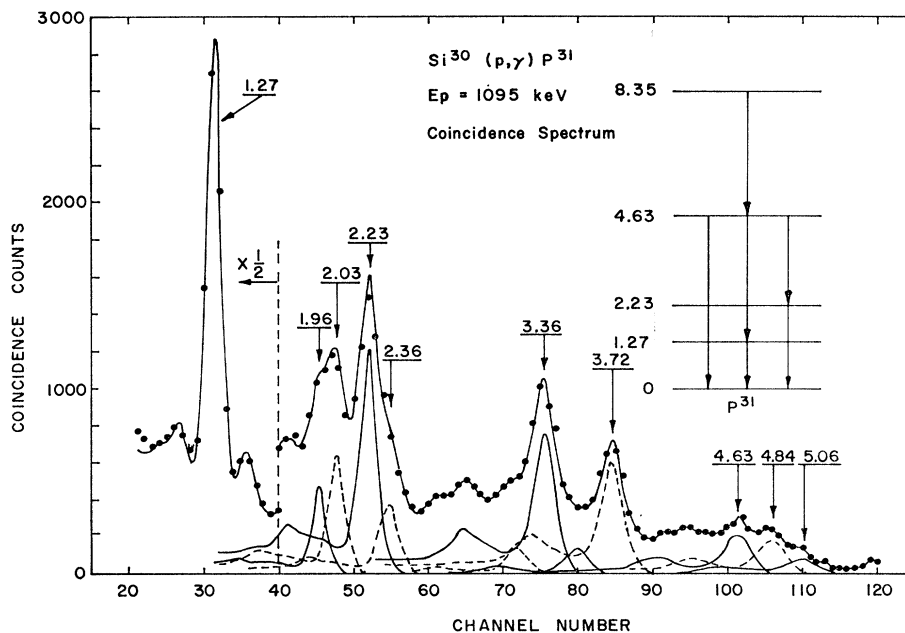


FIG. 15. Singles spectrum at the  $E_p = 1095$  keV resonance obtained with the 8-in.  $\times$  8-in. detector at  $\theta_\gamma = 55^\circ$ . The background contributions have been subtracted automatically as discussed in the text. Some of the most prominent components are shown. The solid curve is the best fit to the data obtained by the spectrum fitting program.

FIG. 16. Spectrum in coincidence with pulses from the portion of the spectrum indicated in Fig. 15 for the  $E_p=1095$  keV resonance. Only the more prominent components are shown. The members of the cascade through the 4.63-MeV level are shown.



moved. A residual peak at 1.4 MeV can be seen which could not be satisfactorily accounted for in the decay scheme.

Some of the more prominent components of this spectrum are shown in Fig. 15. The spectrum analysis was performed in this case by a "stripping" program

TABLE I. Relative intensities (arbitrary units) of gamma rays observed at the  $E_p=1095$  keV resonance. D. S. refers to the intensity used to derive a consistent decay scheme. The listed energies are values computed from the level scheme.

$E_\gamma$ (MeV)	Observed intensity	D.S. intensity
1.06	17.4	22.0
1.27	258.2	285.0
1.46 <sup>a</sup>	26.2	...
1.65 <sup>b</sup>	24.1	8.0
1.96	39.4	40.2
2.03	42.5	46.1
2.23	77.0	66.0
2.36	18.3	14.0
2.58	10.2	11.0
2.69	14.3	11.6
2.92	6.6	8.6
3.13	13.9	13.5
3.36	35.0	31.0
3.51	22.1	25.9
3.57		
3.72	56.9	66.0
4.09	7.8	5.0
4.16	14.8	16.8
4.26		
4.50	12.4	11.0
4.63	25.0	21.0
4.84	24.8	28.0
5.06	49.6	52.1
5.3	6.2	4.5
5.66	10.9	11.6
6.12	24.4	24.4
7.08	188.8	190.0

<sup>a</sup> Presumed due to incomplete compensation for  $K^{40}$  background.  
<sup>b</sup> Intensity discrepancy possibly due to incomplete compensation for contaminant radiation from the  $Na^{23}(p,\gamma)Ne^{20}$  resonance at  $E_p=1090$  keV.

recently developed in this laboratory.<sup>26</sup> The spectrum proved to be considerably more complex than originally suspected or than reported by Van Rinsvelt and Smith. The relative intensities resulting from this analysis and those used in deriving the decay scheme shown in Fig. 17 are listed in Table I. An important factor in the determination of whether the 5.01- or the 4.63-MeV level is predominantly involved is the relative intensities of the 3.36-, 3.72-, 4.63-, and 5.06-MeV gamma rays

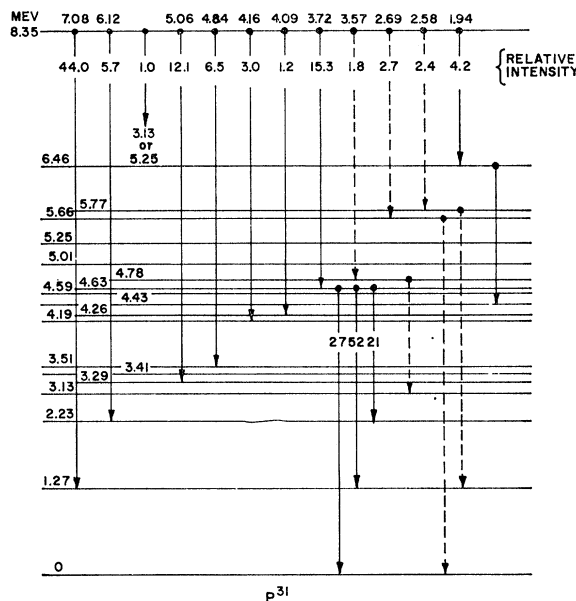


FIG. 17. Proposed decay scheme for the  $E_p=1095$  keV resonance and the 4.63-MeV level.

<sup>26</sup> H. D. Graber and D. D. Watson, Nucl. Instr. Methods (to be published).

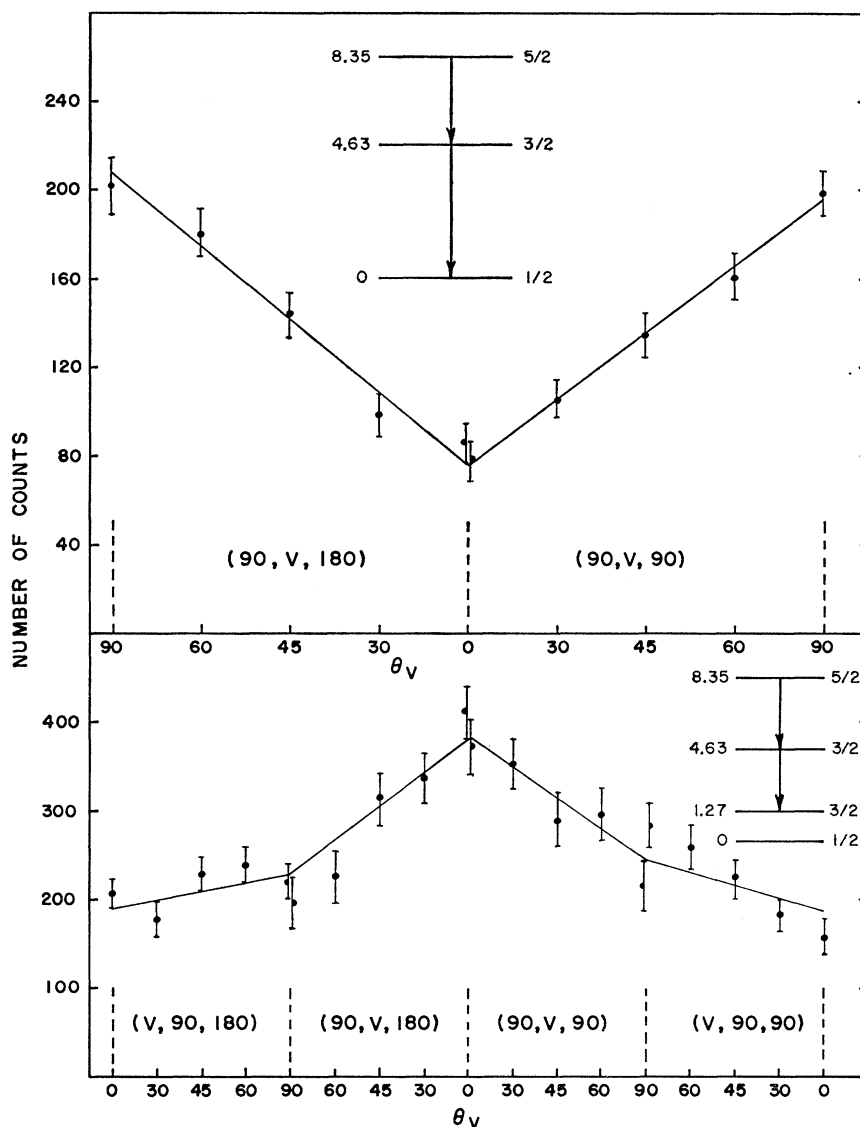


FIG. 18. Angular-correlation data for the  $r \rightarrow 4.63 \rightarrow 0$  and  $r \rightarrow 4.63 \rightarrow 1.27$  cascades from the  $E_p = 1095$  keV resonance. The normalization and fitted curves are for  $J(4.63) = \frac{3}{2}$ .

which are satisfactorily explained only if it is assumed that the resonance decays to the 3.29- and 4.63-MeV levels as shown. Although the resolution is not sufficient to eliminate the possibility that it is the 4.59-MeV level rather than the 4.63-MeV level which is excited, the 4.59-MeV level has been reported earlier to decay only to the 3.29-MeV level.<sup>3,4</sup> It is found that the 4.63-MeV level must decay to the ground, first-excited, and second-excited states. The latter transition has an energy of 2.36 MeV and shows up as a hump on the side of the stronger component in the spectrum at 2.23-MeV. This  $4.63 \rightarrow 2.23$  transition is shown to somewhat better advantage in Fig. 16 which results from adding 80 coincidence spectra obtained during the course of triple-correlation measurements discussed below. The location of the coincidence window used to obtain this spectrum is indicated in Fig. 15. The relative intensities,

corresponding to an average of the results in the singles and coincidence spectra, for the  $4.63 \rightarrow 0$ ,  $4.63 \rightarrow 1.27$ , and  $4.63 \rightarrow 2.23$  transitions are  $27 \pm 4$ ,  $52 \pm 4$ , and  $21 \pm 6\%$ , respectively.

#### *Spin of the 4.63-MeV Level*

During a continuous 48-h run, the triple-correlation data shown in Fig. 18 was obtained for the  $r \rightarrow 4.63 \rightarrow 0$  and  $r \rightarrow 4.63 \rightarrow 1.27$  cascades from the 1095-keV resonance. The setup of Fig. 1 was used to permit the simultaneous measurement of all geometries shown. A total of 8 passes of the movable detector through the angles  $\theta_V$  were performed in order to minimize systematic errors.

The results of the analysis of the two geometries for the  $r \rightarrow 4.63 \rightarrow 0$  cascade are shown in the upper part of

TABLE II. Summary of results of the present study of the 3.29-, 3.51-, 4.26-, and 4.63-MeV levels of  $P^{81}$ . For comparison, the recent results of Van Rinsvelt<sup>a</sup> are also given.

Level energy (MeV)	Spin	Transition	Branching ratio (%)		Multipolarity mixing ( $\delta$ )	
			Present study	Van Rinsvelt	Present study	Van Rinsvelt
3.29	$\frac{5}{2}$	3.29 $\rightarrow$ 0	$0.8 \pm 1.2$	$\leq 1$	...	...
		3.29 $\rightarrow$ 1.27	$77 \pm 2$	$82 \pm 5$	$-0.44 \pm 0.02$	$-0.37 \pm 0.02$
		3.29 $\rightarrow$ 2.23	$23 \pm 2$	$18 \pm 5$	$-0.41 \pm 0.06$	$-0.05 \pm 0.06$
3.51	$\frac{3}{2}$	3.51 $\rightarrow$ 0	$64 \pm 3$	$70 \pm 5$	$-0.41 \pm 0.03$	$-0.43 \pm 0.03$
		3.51 $\rightarrow$ 1.27	$20 \pm 14$	$30 \pm 5^b$	7.1 $\pm 1.0$	8.2 $\pm 1.8$
		3.51 $\rightarrow$ 2.23	$16 \pm 14$		$\left\{ \begin{array}{l} 0.06 \pm 0.19 \\ -0.05_{-0.11}^{+1.05} \end{array} \right.$	
4.26	$\frac{3}{2}$	4.26 $\rightarrow$ 0	$76 \pm 3$		$-0.32 \pm 0.04$	
		4.26 $\rightarrow$ 1.27	$20 \pm 3$		4.7 $\pm 0.9$	
		4.26 $\rightarrow$ 2.23	$4 \pm 3$		$-0.25 \pm 0.05$	
4.63	$\frac{3}{2}$	4.63 $\rightarrow$ 0	$27 \pm 4$	20	$0.07 \pm 0.04$	
		4.63 $\rightarrow$ 1.27	$52 \pm 4$	80	$1.48 \pm 0.12$	$-0.02 \pm 0.05$
		4.63 $\rightarrow$ 2.23	$21 \pm 6$	...	$-3.9 \pm 1.0$	...

<sup>a</sup> Reference 27.<sup>b</sup> This value represents the combined intensities for the 3.51  $\rightarrow$  1.27 and 3.51  $\rightarrow$  2.23 transition.

Fig. 19. The projections of the  $Q^2$  surfaces are shown for the assumptions  $J(4.63) = \frac{3}{2}, \frac{5}{2},$  and  $\frac{7}{2}$ . The spin- $\frac{5}{2}$  result of Van Rinsvelt and Smith for the resonance is used. The minimum value of  $Q^2$  for  $J(4.63) = \frac{1}{2}$  was 29.6. It is clear that the 4.63-MeV level must have  $J = \frac{3}{2}$ . This conclusion was verified by the analysis of the data on the  $r \rightarrow 4.63 \rightarrow 1.27$  cascade. The result of this analysis for  $J(4.63) = \frac{3}{2}$  is shown in the lower part of Fig. 19. The agreement of the values of  $\delta_{r \rightarrow 4.63}$  obtained from the two cascades can be seen to be very good. The weighted average is  $-0.07 \pm 0.03$ . The two possible values of  $\delta$  for the 4.63  $\rightarrow$  0 transition are  $0.07 \pm 0.04$  or  $1.48 \pm 0.12$ . Similarly, the two possible values of  $\delta$  for the 4.63  $\rightarrow$  1.27 transition are  $-0.02 \pm 0.05$  or  $-3.9 \pm 1.0$ .

### SUMMARY AND DISCUSSION

Prior to the present work, the spin assignments for the 3.29-, 3.51-, and 4.26-MeV levels of  $P^{81}$  were based primarily upon  $(p, \gamma)$  angular-distribution measurements, and the properties of the 4.63-MeV level were not known. The development of the more efficient experimental and data analysis techniques introduced in this paper for  $(p, \gamma, \gamma)$  triple-correlation measurements has allowed a much more exhaustive examination of all physically reasonable spin values for these levels. Unique spin assignments were obtained for all four levels and earlier assignments were confirmed. A primary aim of this work was to investigate the electromagnetic transitions from these four bound states. Considerable detailed and more precise information was obtained on branching and multipolarity-mixing ratios. The measurements pertaining to the 4.63-MeV level were performed at the  $E_p = 1095$  keV resonance which

was found to have decay properties significantly different from those reported in the literature. A detailed study of the resonance was thus undertaken and the

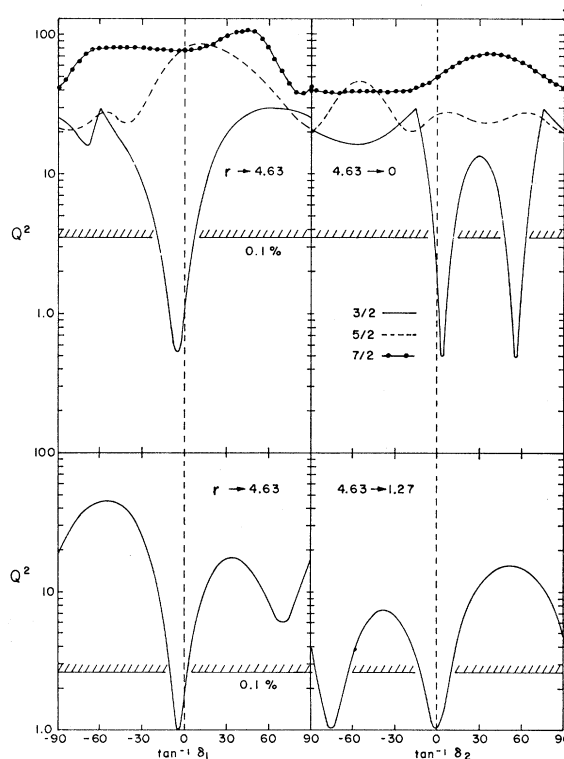


FIG. 19. Projection plots of the  $Q^2$  surfaces for the data of Fig. 18 for cascades from the  $E_p = 1095$  keV resonance. The upper curves are for the  $r \rightarrow 4.63 \rightarrow 0$  cascade, and the lower are for the  $r \rightarrow 4.63 \rightarrow 1.27$  cascade.

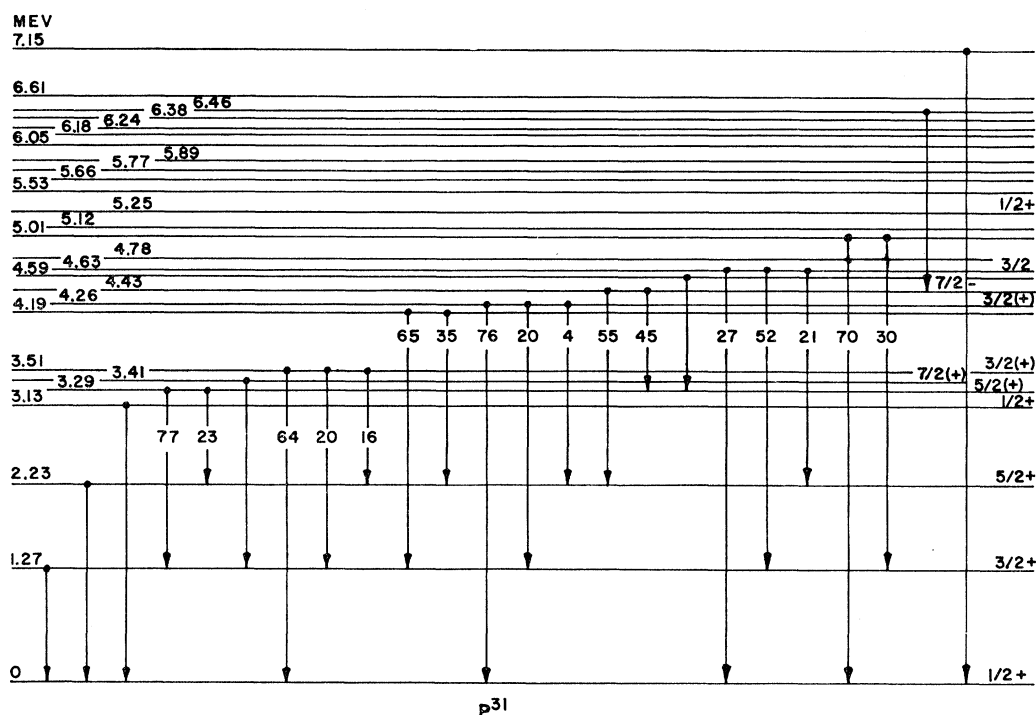


FIG. 20. Decay scheme summarizing the decay properties and some of the known spin and parity assignments of bound levels of  $P^{31}$ . The spins and decay schemes of the 3.29-, 3.51-, 4.26-, and 4.63-MeV levels result from the present study. The properties of the 1.27-, 2.23-, 4.19-, and 4.59-MeV levels are taken from Ref. 7. The energies of the levels up through 5.01 MeV are also from this reference. The level energies above 5.01 MeV are from Ref. 13. (See also Ref. 12.) The properties of the 3.13-MeV level are taken from Refs. 8 and 13, those for the 3.41-MeV level from Refs. 5 and 6, those for the 5.01- and 6.46-MeV levels from Ref. 5, those for the 4.43-MeV level from Refs. 9 and 16, and those for the 7.15-MeV level are taken from Ref. 28. Multipolarity mixings measured in the present study are listed in Table II. *Note added in proof.* Recent measurements by Davies, Dawson, and Neilson [Phys. Letters **19**, 576 (1965)] using the  $Si^{30}(d,n)P^{31}$  reaction lead to the assignments  $\frac{3}{2}^-$ ,  $\frac{3}{2}^+$ ,  $\frac{3}{2}^-$ ,  $(\frac{3}{2}^-, \frac{3}{2}^-)$ , and  $\frac{3}{2}^+$  for the 5.01-, 6.38-, 6.46-, 6.61-, and 7.15-MeV levels, respectively. The assignment  $6.46(\frac{3}{2}^-)$  casts doubt upon the  $6.46 \rightarrow 4.43$  transition shown. Thus proposed cascades through the 6.46-MeV level from resonances in  $Si^{30}(p,\gamma)P^{31}$  may be in need of revision.

results are summarized in Fig. 17. The results of the present work on the 3.29-, 3.51-, 4.26-, and 4.63-MeV levels of  $P^{31}$  are summarized in Table II. In addition, for purposes of review the bound level structure of  $P^{31}$  is shown in Fig. 20.

During the final stages of preparation of the manuscript, the thesis of Van Rinsvelt<sup>27</sup> was received which includes a chapter on a similar study of the 3.13-, 3.29-, 3.41-, and 3.51-MeV levels of  $P^{31}$ . Thus it is possible to compare results for the 3.29- and 3.51-MeV levels. This comparison is made in Table II. The spin assignments are in agreement for the two levels. It can be seen that the branching ratios for the decay of the 3.29- and 3.51-MeV levels are in good agreement. However, from his triple-correlation measurements at the 1770-keV resonance, Van Rinsvelt was unable to obtain any information on the  $(3.29 \rightarrow 1.27)/(3.29 \rightarrow 2.23)$  branching ratio. Where they can be compared, the multipolarity mixings are in reasonable agreement except that for the  $3.29 \rightarrow 2.23$  transition. The difference

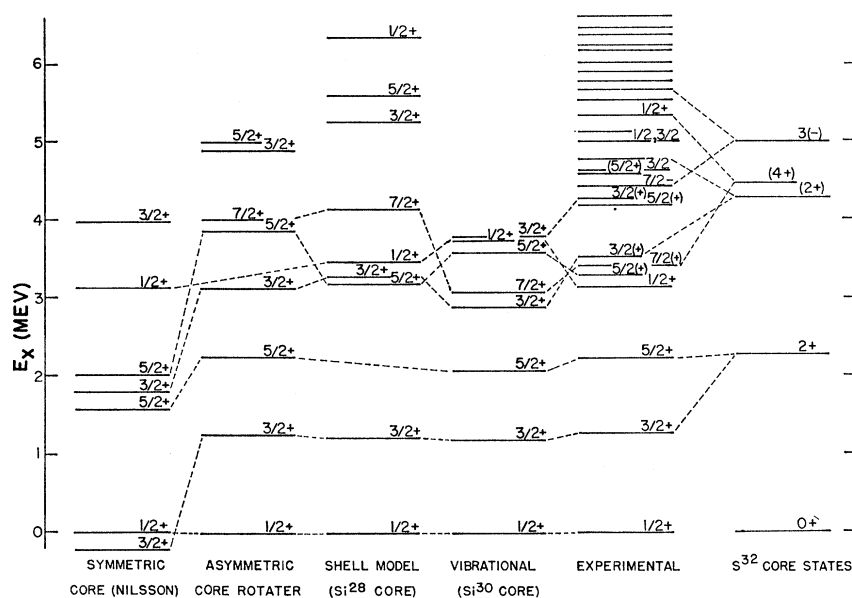
between the values is much greater than the quoted errors. The explanation for this discrepancy is unknown; however, it is probably related to the fact that the intensity of the 1.06-MeV,  $3.29 \rightarrow 2.23$  transition is rather difficult to extract properly from the coincidence spectra because of the nearby strong 1.27-MeV gamma ray from the first-excited state (see Fig. 2). In the triple-correlation measurements reported here, this effect was deliberately minimized by the use of "compensating windows" set just above the 2.23-MeV gamma ray in the spectrum. The subtraction of the "compensation spectra" thereby obtained from the appropriate coincidence spectra results in a spectrum having very little of the interfering 1.27-MeV gamma ray. Van Rinsvelt also presents, without further discussion, a decay scheme of the  $E_p = 1660$ -keV resonance which shows a 10% transition to the 4.63-MeV level. The 4.63-MeV level is shown as decaying in the ratio 20:80 to the ground and first-excited states. These results are also included in Table II for comparison.

The ambiguities in the values of  $\delta$  for the ground-state transitions from the spin- $\frac{3}{2}$  levels cannot be removed by intensity-direction correlation measurements.<sup>5,6,15</sup> However, they could in principle be re-

<sup>27</sup> H. A. Van Rinsvelt, thesis, University of Utrecht, 1965 (to be published).

<sup>28</sup> P. F. Hinrichsen and C. P. Swann, Phys. Rev. **140**, B549 (1965).

FIG. 21. Comparison of the results of various model calculations with the experimental level scheme of  $P^{31}$ . The presumed correspondences between levels are denoted by dashed lines. See text for discussion and references.



moved by means of polarization-direction correlation measurements. The ambiguity in  $\delta$  for the  $4.63 \rightarrow 1.27$  transition could be removed by triple-correlation measurements on the  $4.63 \rightarrow 1.27 \rightarrow 0$  cascade. This measurement was not attempted in this work because of the complexity and weakness of the  $E_p = 1095$  keV resonance. For similar reasons, no attempt was made to measure the mixing ratio for the  $4.63 \rightarrow 2.23$  transition.

It was found in this work that the information which can be obtained from triple-correlation measurements is considerably greater if use is made of the extended formalism for multiple cascades. For example, ambiguities in  $\delta$  can be removed in transitions (to states other than the ground state) from intermediate levels with spin less than two by the technique of measuring the triple correlation of the second and third members of a triple cascade. This cannot be done by measurements on the first two members alone of the same cascade. An example of the usefulness of a flexible triple-correlation formalism for multiple cascades is provided in this work by the analysis of the decay scheme of the 3.51-MeV level. These techniques are now being applied to additional measurements on  $P^{31}$  and other  $1d-2s$  shell nuclei.

A number of calculations based upon several theoretical models have been performed which relate directly to levels in  $P^{31}$ . It seems useful to compare, where possible, the results of some of these calculations with the experimental level scheme which includes the results of the present study. Some of the more recent calculations are those based upon a weak-coupling unified model by Thankappan,<sup>29</sup> the Nilsson model by Bishop, Bottino, and Lombard,<sup>30</sup> the asymmetric-core

rotator model by Chi and Davidson,<sup>31</sup> and shell-model calculations by Glaudemans, Wiechers, and Brussaard<sup>32</sup> who consider an inert  $Si^{28}$  core with two-particle interaction between the nucleons in the  $2s_{1/2}$  and  $1d_{3/2}$  shells. Also, attempts have been made to identify levels in  $P^{31}$  as  $2s_{1/2}$  hole states in an excited  $S^{32}$  core. Such a weak-coupling model has been applied, for example, by Crawley.<sup>12</sup> The level spectra resulting from these calculations are shown in Fig. 21 along with the experimental level scheme. Although we choose here not to give a detailed discussion of each of these calculations, some results of each seem worthy of comment.

The calculations of Thankappan assume weak coupling between intrinsic states of the odd proton and the vibrational modes of the  $Si^{30}$  core. Core vibration modes through three phonons are included. The resulting level spectrum is seen to agree quite well with the observed levels below 4 MeV. Electromagnetic transition probabilities obtained from this model appear to be in better agreement with data than implied in Thankappan's paper for the following reasons: Among the transition probabilities he calculated are those for the decay of the second lowest  $\frac{3}{2}^+$  state (referred to as  $\frac{3}{2}^*$ ) to the states at 0, 1.27, and 2.23 MeV. At the time of these calculations it was thought that the 3.13-MeV level was  $\frac{3}{2}^+$ , and it was therefore identified by Thankappan with  $\frac{3}{2}^*$ . For the value 10 MeV for the model parameter  $k$ , which is chosen to provide a reasonable fit to the rest of the data, he finds that the  $\frac{3}{2}^*$  level decays in the ratio 55:18:27 to the 0-, 1.27-, and 2.23-MeV levels, respectively. The 3.13-MeV level, however, decays by at least 99% to the ground state.<sup>27</sup> Subsequent to these calculations, it has been shown<sup>8,18</sup>

<sup>29</sup> V. K. Thankappan, Phys. Letters 2, 122 (1962).

<sup>30</sup> G. R. Bishop, A. Bottino, and R. M. Lombard, Phys. Letters 15, 323 (1965).

<sup>31</sup> B. E. Chi and J. P. Davidson, Phys. Rev. 131, 366 (1963).

<sup>32</sup> P. W. M. Glaudemans, G. Wiechers, and P. J. Brussaard, Nucl. Phys. 56, 548 (1964).

that the 3.13-MeV level has spin and parity  $\frac{1}{2}+$ . The  $\frac{3}{2}^*$  level of Thankappan should therefore be identified with the 3.51-MeV level studied in the present work. The experimental branching ratio from this state to the lowest three states was found to be 64:20:16 in very good agreement, considering the errors, with the calculated ratio. For  $k=10$  MeV, the magnitudes of the multipolarity mixing ratios for the  $3.51 \rightarrow 0$ ,  $3.51 \rightarrow 1.27$ , and  $3.51 \rightarrow 2.23$  transition are computed from Thankappan's transition probabilities to be  $\delta=8.9$ ,  $0.76$ , and  $0.04$ , respectively. The agreement with the observed mixing ratios listed in Table II is seen to be remarkably good if the high value for  $\delta(3.51 \rightarrow 0)$  is chosen. (A polarization measurement to determine uniquely the latter mixing ratio would be a useful test of this model.) Finally, the absolute  $E2$  transition probability  $T(E2)=35.9 \times 10^{12} \text{ sec}^{-1}$  calculated by Thankappan for  $k=10$  MeV is in reasonable agreement with a value  $T(E2)=5.9 \times 10^{12} \text{ sec}^{-1}$  computed from the high-energy electron scattering data of Kossanyi-Demay *et al.*<sup>10</sup> It should be pointed out, however, that for  $k=10$  MeV the mixing ratio for the decay of the 1.27-MeV level is  $\delta=7.8$  as opposed to the experimental value of  $0.28$ .<sup>5,6</sup> This discrepancy can be attributed to the fact that the theoretical  $M1$  transition probability is a factor of 300 too low.

The strong-coupling (Nilsson) model calculations of Bishop *et al.*<sup>30</sup> differ from previous symmetric-core Nilsson model calculations by Broude *et al.*,<sup>3</sup> and a later revised version discussed in II, in that the 3.13-MeV level is identified with Nilsson orbit No. 11 instead of with the second member of Nilsson orbit No. 9. This new identification was prompted by results of the inelastic scattering data mentioned above and the new assignment of spin  $\frac{1}{2}$  to the 3.13-MeV level. The resulting level spectrum shown in Fig. 21 corresponds to a particular choice of model parameters. Other choices of parameters led to equally poor agreement with the experimental level scheme. It is seen that the model does not reproduce the correct sequence for even the lowest levels. The authors consequently conclude that the level scheme of  $P^{31}$  would be difficult to explain on the basis of the (symmetric-core) Nilsson model. A better agreement with the experimental level scheme was obtained by Chi and Davidson<sup>31</sup> with a modified form of the strong-coupling Nilsson model in which the extra nucleon is assumed to be coupled to an asymmetric, rotating core. This model, although apparently more successful than the symmetric-core version, fails to predict a level of spin  $\frac{1}{2}$  below 5 MeV. No computed electromagnetic properties have been reported for either of these strong-coupling models.

The shell-model calculations of Glaudemans *et al.*<sup>32</sup> involve the fifteen interaction energies of two-particle configurations and the binding energies (to a  $Si^{28}$  core) of  $2s_{1/2}$  and  $1d_{3/2}$  nucleons as parameters which are

determined by a least-squares fitting procedure. In this procedure, the computed energies are compared with energies of fifty states in the region  $28 < A \leq 40$  with known spin and isospin. From the best values of the seventeen parameters thereby obtained, the energies and wave functions of 377 states in this region were calculated. The resulting level spectrum for  $P^{31}$  is reproduced in Fig. 21. The calculated spectrum is seen to agree well with energies of states below 3.5 MeV except that the  $\frac{5}{2}+$  level at 2.23 MeV is not reproduced. The authors conclude, therefore, that the 2.23-MeV level probably arises from excitation of the  $Si^{28}$  core. Wiechers and Brussaard,<sup>33</sup> using the wave functions obtained with this model, have calculated the level widths for  $M1$  transitions to the ground state of  $P^{31}$  from the 1.27- and 3.13-MeV levels. The result for the 3.13-MeV level is in close agreement with the experimental value, whereas that for the 1.27-MeV level is about a factor of 60 too low.

Attempts have also been made to identify states in  $P^{31}$  as  $2s_{1/2}$  hole configurations weakly coupled to  $S^{32}$  core excitations. An example of such an identification is taken from the work of Crawley<sup>12</sup> who observed the inelastic scattering of 17.5-MeV protons from  $P^{31}$  and  $S^{32}$ . One assumes there should be pairs of levels in  $P^{31}$  which result from the coupling of a  $1s_{1/2}$  hole to collective states in  $S^{32}$ . The four strongly excited states observed by Crawley in  $S^{32}$  are shown to the right of the experimental level scheme in Fig. 21. The dashed lines indicate a suggested coupling scheme for states in  $P^{31}$ . This assignment was made by Crawley on the basis of the similarity of angular distributions for the corresponding states, and on the basis of known spins and parities of levels in both nuclei. This is the only model to be considered so far which provides an explanation for the observed<sup>9,22</sup>  $\frac{7}{2}-$  level at 4.43 MeV. If the identification shown is correct, then the level at 5.66 MeV would be expected to be  $\frac{5}{2}-$ . This interpretation is supported by the inelastic electron scattering work<sup>10</sup> in which  $E3$  excitation of a level at  $5.67 \pm 0.07$  MeV in  $P^{31}$  is observed. The model proposed also predicts  $\frac{5}{2}+$  and  $\frac{3}{2}+$  for levels at 4.78 and 5.34 MeV, respectively. Subsequent measurements, however, by Cujec *et al.*<sup>13</sup> using the  $Si^{30}(d,n)P^{31}$  reaction yield  $l_p=0$ , thus  $J^\pi=\frac{1}{2}+$ , for the 5.25-MeV level which is probably the "5.34-MeV level" of Crawley. An alternative coupling scheme proposed by Crawley predicts  $\frac{3}{2}+$  and  $\frac{5}{2}+$  for the 4.78- and 5.34-MeV levels, respectively. Thus it seems that the coupling based upon a possible  $4+$  level at 4.47 MeV in  $S^{32}$  should be re-examined.

It appears that, on the basis of comparison between results of the available model calculations, the weak-coupling unified models receive greater support from the existing data on  $P^{31}$  than do the other models.

<sup>33</sup> G. Wiechers and P. J. Brussaard, Nucl. Phys. **73**, 604 (1965).

There is now even stronger support for an earlier assertion<sup>5</sup> to the effect that the established rotational structure near  $A=25$  becomes less pronounced, and in fact gives way to weak-coupling vibrational structure in the region near  $A=30$ . It is clear, however, that the more realistic test for any of these models lies in the agreement between computed and measured dynamic properties such as the absolute radiative transition probabilities, branching ratios, and multipolarity mixings. There remains a scarcity of both data and calculations of these parameters even for the nucleus presently considered.

#### ACKNOWLEDGMENTS

The measurements discussed in this paper have extended over a period of several years and, consequently, several people were involved at various times in the operation of the accelerator and in the analysis of data. We thank each of them and especially W. A. Anderson, A. K. Hyder, and D. D. Watson who contributed freely of their time to machine operation. We also thank Lt. Hyder and Dr. Watson for their continuing advice and efforts in the development of the appropriate computer programs, and Dr. H. J. Hennecke for a critical reading of the manuscript.

### Elastic and Inelastic Scattering of 9.8-MeV Deuterons from $P^{31}\dagger$

B. T. LUCAS AND O. E. JOHNSON

*Department of Physics, Purdue University, Lafayette, Indiana*

(Received 7 January 1966)

The 9.8-MeV differential cross sections for deuteron scattering reactions which leave  $P^{31}$  in its ground and lowest three excited states (1.265, 2.232, and 3.133 MeV) have been measured. The targets were produced by the vacuum evaporation of red phosphorous ( $\sim 625 \mu\text{g}/\text{cm}^2$ ) onto thin Formvar films ( $2-5 \mu\text{g}/\text{cm}^2$ ). The spectra were measured using an electronic mass-discriminating spectrometer system which incorporated an  $(E, \Delta E)$  counter telescope consisting of two silicon surface-barrier detectors. The  $(\sigma_E/\sigma_R)$  ratio for the elastic scattering exhibits a somewhat irregular oscillatory structure forward of  $100^\circ$ . The  $d_1$  and  $d_2$  angular distributions are remarkably similar in shape and are clearly in phase, but there is no definite phase relationship between them and the  $d_0$  angular distribution. The  $d_3$  angular distribution is roughly out of phase with the  $d_1$  and  $d_2$  angular distributions. The integrated cross sections for the excitation of the first, second, and third excited states are  $3.51 \pm 0.04$  mb ( $26.7^\circ-170.7^\circ$ ),  $6.74 \pm 0.04$  mb ( $26.8^\circ-170.7^\circ$ ), and  $0.77 \pm 0.02$  mb ( $32.3^\circ-170.8^\circ$ ), respectively. The elastic-scattering cross section was analyzed in terms of the nuclear optical model with a four-parameter Saxon potential. Three distinct sets of parameters were found which give moderately good fits to the experimental data for angles less than  $150^\circ$ . The ambiguities in the optical-model parameters encountered in the fitting procedure are described and discussed. The  $d_1$  and  $d_2$  cross sections were analyzed in terms of the distorted-wave theory using a simple collective-model description for the excited states of  $P^{31}$  and the optical-model parameters determined through the analysis of the elastic-scattering data. The resulting calculated cross sections reproduce the general features of the data over a rather wide angular range, the most serious discrepancies occurring at forward angles. The implications of these analyses and the present experimental results are discussed in terms of existing collective-model descriptions of this nucleus.

#### I. INTRODUCTION

UNTIL recently the spins, parities, and spacings of the low-lying levels of  $P^{31}$  had been presumed to be well established.<sup>1</sup> A number of theoretical studies of this nucleus had been made within the framework of the Nilsson<sup>2,3</sup> and weak-coupling<sup>4,5</sup> models in which the

previous spin and parity assignments were assumed to be valid. None of these studies provided a completely satisfactory description of the levels and decay properties of this nucleus. Recently, experimental measurements were reported<sup>6,7</sup> which indicate that the assignment of  $\frac{3}{2}^+$  for the 3.133-MeV state is incorrect and should be  $\frac{1}{2}^+$ . This assertion prompted theoretical reconsideration. A re-identification of the levels was undertaken in terms of the Nilsson model; however, the resulting level scheme is described as being in serious

<sup>†</sup> Work supported in part by the U. S. Atomic Energy Commission.

<sup>1</sup> Unless otherwise specified, the level structure and individual level properties proposed for  $P^{31}$  in the following compilation will be assumed: P. N. Endt and C. Van Der Leun, Nucl. Phys. **34**, 1 (1962). In cases where specific quantitative information and/or interpretations are under discussion, a full bibliographical reference to the original reports will be made.

<sup>2</sup> C. Broude, L. L. Green, and J. C. Willmott, Proc. Phys. Soc. (London) **72**, 1097 (1958).

<sup>3</sup> L. L. Green, J. C. Willmott, and G. Kayne, Nucl. Phys. **25**, 278 (1961).

<sup>4</sup> V. K. Thankappan, Phys. Letters **2**, 122 (1962).

<sup>5</sup> V. K. Thankappan and S. P. Pandya, Nucl. Phys. **19**, 303 (1960).

<sup>6</sup> H. A. Van Rinsvelt and P. M. Endt, Phys. Letters **9**, 266 (1964).

<sup>7</sup> B. Cujec, W. G. Davies, W. K. Dawson, T. B. Grandy, G. T. Neilson, and K. Ramavaram, Phys. Letters **15**, 266 (1965).